Utrecht University
Faculty of Geosciences
Department of Physical Geography

BACHELOR THESIS

Universiteit Utrecht

Man-made blowout sites in the foredunes of Zuid-Kennemerland: a comparison to coastal trough blowouts

Author: E.P. van Onselen
Student ID: 4007069
1st supervisor: Prof. Dr. Gerben Ruessink
2nd supervisor: Jasper Donker MSc.

UTRECHT, July 2015

Contents

Abstract

In the foredunes at Zuid-Kennemerland national park, The Netherlands, five trenches were made to promote sediment transport from the beach to the dune valleys behind the foredune ridge. The man-made trenches bear a close resemblance to trough blowouts, a naturally-occuring aeolian feature common in coastal dune areas. In this study, I compared the trenches of Zuid-Kennemerland to natural trough blowouts in terms of morphology, evolution, flow dynamics and erosional/depositional patterns. A total of four digital elevation models, made between April 2014 and April 2015, were analyzed for this study. Both visual interpretations and quantitative data retrieved from the DEMs were combined with current knowledge of natural trough blowouts and up-to-date meteorological data. It appears that the man-made trenches are important pathways of sediment transport. Erosion is dominant within the deflation basin and especially on the sidewalls, whereas sediment is deposited closely behind the deflation basin area. Erosional and depositional patterns show a good correlation with dominant wind direction and speed. The morphology and evolution of the trenches are, however, different from natural trough blowouts. The trenches are relatively wide compared to their natural counterparts. In addition, the trenches do not have a clear transportational ramp, which means that the depositional lobe often lies downhill from the deflation basin. Hence, it is difficult to make an accurate model of flow dynamics within and around the trenches without conducting a field study.

KEY WORDS: trough blowouts, foredunes, flow dynamics, aeolian transport, dune management

1. Introduction

Dune management on the Dutch coast traditionally focused on erosion control through active maintenance of the foredune ridge by means of e.g. nourishments and marram planting (Klijn, 1990; Provoost *et al.*, 2011). This led to overstabilization of the foredune area, reducing sand supply to the area on the lee side of the foredune ridge. The stabilized dune area leads to a decrease in pioneer vegetation as vegetation quickly succeeds towards its climax stage (Provoost *et al.*, 2011). In addition, the inactive grey dunes undergo accelerated acidification, decreasing biodiversity (Kuipers, 2014). Since the 1970s there has been a growing awareness of the importance of a dynamic dune system (Arens *et al.*, 2013). Present dune management projects therefore often focus on dune remobilization.

In the coastal dunes of Zuid-Kennemerland National Park, The Netherlands, the dune remobilization project 'Noordwest Natuurkern' has recently been initiated (Kuipers, 2014). Five trenches were cut through the foredune in order to promote sand transport from the beach to the damp dune valley and parabolic dunes behind the foredune ridge. Enhanced transport and distribution of lime on the coastal plain should improve conditions for lime-rich habitats and species (Kuipers, 2014). Although primarily an ecological project, it is also of paramount importance that the effect of these trenches on sediment transport patterns is studied. This may help to improve our understanding of dune revival projects and their effects on both ecology and coastal defence. The trenches are very similar to natural trough blowouts, a common feature in coastal dune systems (See e.g. review of Hesp, 2002). The degree of resemblance in terms of morphology, airflow dynamics and sediment transport has not yet been investigated. Understanding the similarities and differences between the trenches and coastal trough blowouts may potentially help to improve our understanding of the artificial blowouts and may help in improving their design. It is therefore of critical importance that the relation of the artificial trenches to natural trough blowouts is fully understood.

A previous study by Arens *et al.* (2004) focused on the development of a remobilized parabolic dune a few kilometers landward from the trenches. They concluded that remobilization by the removal of vegetation has been successful, yet active maintenance by repeated vegetation removal was necessary. Similar parabolic dune reactivation projects were carried out at different locations and also showed that recurring removal of vegetation is necessary to sustain dynamic dune development (Kuipers, 2014). Other studies addressed the morphological evolution of natural trough blowouts by applying remote sensing techniques (e.g. Dech *et al.*, 2005; Gonzalez-Villanueva *et al.*, 2011). These studies focused primarily on spatial development of a trough blowout. Numerous studies have been carried out addressing trough blowout flow dynamics (e.g. Hesp and Hyde, 1996; Fraser *et al.*, 1998; Hesp and Pringle, 2001; Pease and Gares, 2013; Smyth *et al.*, 2014) and sediment transport (e.g. Byrne, 1997). However, there are no studies in which morphological evolution, flow dynamics and sediment transport patterns of a trough blowout are all addressed simultaneously using only remotely sensed data.

In this study I aim to give a better understanding of the man-made trenches at Zuid-Kennemerland and how they compare to natural trough blowouts. I will compare the trenches to natural trough blowouts based on morphology, evolution during a one-year period, sediment transport patterns and their implications on flow dynamics by analyzing Digital Elevation Models (DEMs) and combining the results with our current understanding of trough blowouts.

2. Current understanding of trough blowouts

2.1. Introduction to blowouts

A blowout is a morphological feature that is created by wind erosion of unconsolidated sand in dune systems. In literature, the shape of a blowout is most commonly described as a saucer-, cup- or trough-shaped depression in a pre-existing sand deposit (Hesp and Hyde, 1996). Saucer- and cup-blowouts are shallow, disc-shaped features, whereas a through blowout is characterized by its elongated, trench-like shape and high erosional walls. By definition, trough blowouts are longer than that they are wide (see examples in e.g. Hesp and Hyde, 1996; Hesp, 1996; Byrne, 1997; Fraser *et al.*, 1998; Neal and Roberts, 2001; Hesp, 2002; Pease and Gares, 2013; Smyth *et al.* 2014). A trough blowout may cut through a linear dune ridge (Carter *et al.*, 1990). The blowout is typically aligned with the predominant wind direction (González-Villanueva *et al.*, 2011). The blowout entrance is located on the windward side of the blowout and is followed by the deflation basin further downwind. The central part of the deflation basin, where most of the material is removed, is sometimes referred to as the deflation floor. On either side of the deflation basin there are sidewalls that typically have a straight to slightly concave upward slope. The sidewalls are bounded by the 'rim', which sometimes features small dunes if there is a sufficient amount of spillover deposits. The rim marks the boundary of the blowout. Further downwind from the deflation basin, there is a ramp leading up to depositional lobe. This ramp is called 'the transportational ramp' and is an important link that accommodates sediment transfer between the erosional deflation basin and depositional lobe. An overview of the main morphological features of a trough blowout is given in Figure 1.

Blowouts may be found in a wide range of environments that feature sand dunes. Blowouts may develop on temperate, sandy grasslands (Hugenholtz and Wolfe, 2006; Wang *et al.*, 2007), in deserts and semi-arid environments (Hesp, 2002; Whitney *et al.*, 2015) as well as in (peri-)glacial environments (Adamson *et al.*, 1988). Blowouts are also common in coastal dune systems, especially if the adjacent beach periodically erodes or recedes (Hesp and Hyde, 1996; Hesp, 2002). The morphology of blowouts is highly variable both spatially and temporarily as their initiation and evolution depends on many factors (Hesp, 2002). In this chapter, I attempt to summarize our current understanding of blowouts in coastal dune areas in terms of their initiation, morphology and evolution. I will mainly focus on flow dynamics and sediment transport in trough blowouts by comparing the results of numerous studies on trough blowout morphodynamics.

2.2. Initiation of blowouts

Coastal dune blowouts can be initiated in a variety of ways. According to Hesp and Hyde (1996), many

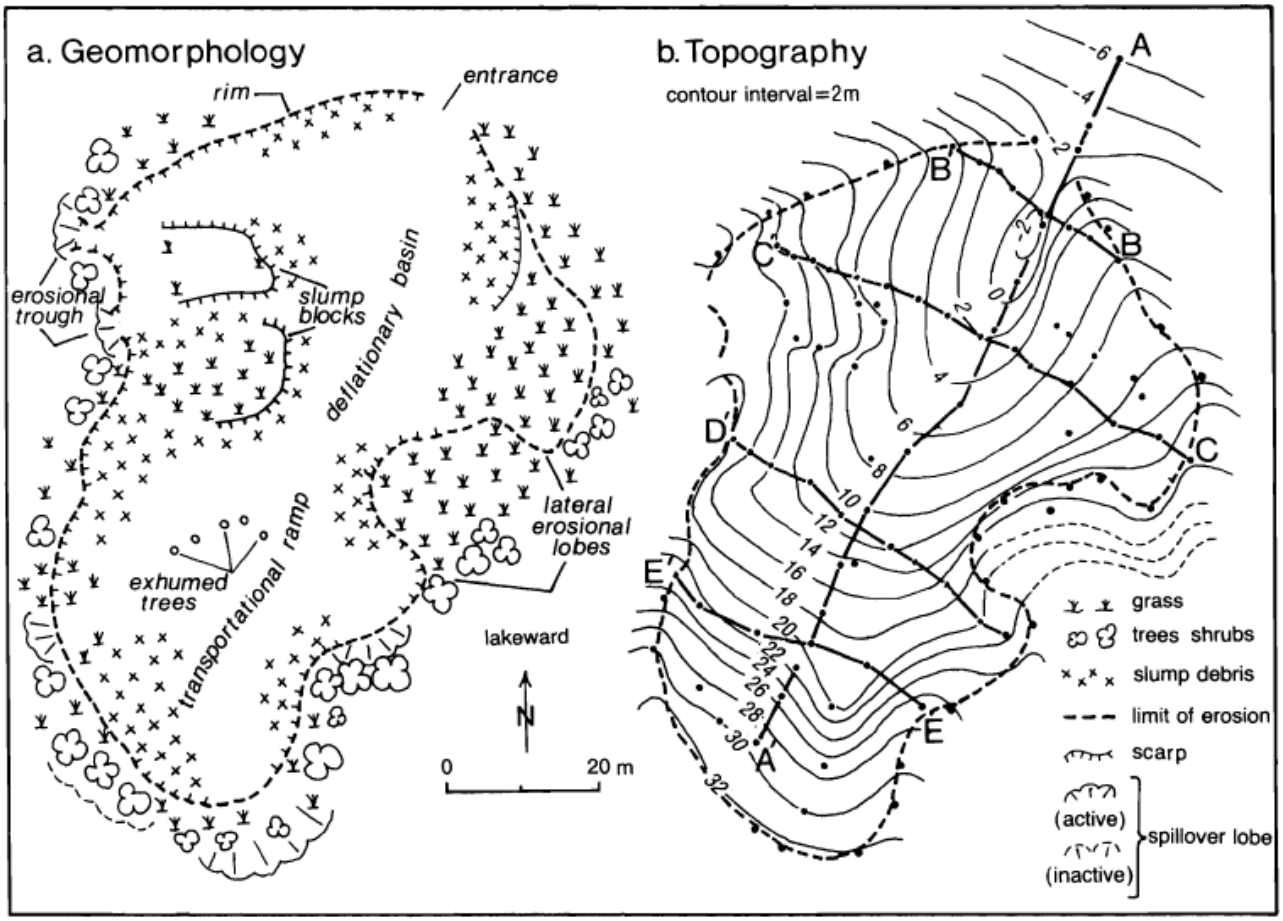

Figure 1. Morphology of a trough blowout on the southern coast of Lake Michigan, IN, USA. The depositional lobe is located below the transportational ramp in this picture, but is not shown in this illustration. (Source: Fraser *et al.*, 1998 pp. 452)

authors agree that a lack or removal of vegetation cover is of critical importance for the initiation of blowouts. Furthermore, González-Villanueva *et al.* (2011) concluded that the initiation of blowouts is also related to pre-existing topography, wind and wave erosion of foredunes. This is conform earlier findings that were reviewed in Hesp (2002). In this review, Hesp identified seven possible causes that contribute to the formation of blowouts: (1) Wave-driven erosion along the foredunes; (2) Topographic acceleration of airflow over dune crests; (3) climate change; (4) spatial and temporal variation in vegetation cover; (5) water erosion; (6) wind erosion and/or deposition (burial of vegetation); and (7) human activities. All of these possible causes decrease the stability of a dune by either removing vegetation, moisture or by altering its dimensions such that the slopes become unstable. If the resulting perturbation is sufficient, aeolian processes will take over to create the actual blowout. Coastal dune blowouts may be initiated on both the seaward and the landward face of a dune by both onshore and/or offshore winds (Gares and Nordstrom, 1995).

(1) Wave-driven erosion may contribute to the formation of blowouts in conjunction with topographic acceleration of airflow. Continuous along-shore wave erosion may cause slumping to occur on the seaward slope of primary dunes. Winds are accelerated in the depression below the scarp face of a slump, marking the onset of blowout development (Hesp, 2002). Slumping may also contribute to the development of blowouts if there are poorly vegetated or depressed weak spots along the scarp crest (Hesp, 2002). Wave erosion may also completely remove the pioneer vegetation zone, thereby exposing the perennial plants, shrubs or even woodlands behind it. Subsequent reduction and retreat of these vegetation types may lead to the development of blowouts (Hesp and Hyde, 1996). Hollows and washover fans created by overwashes may also accommodate the development of blowouts if revegetation is slow enough (Hesp, 2002).

(2) A blowout can also be initiated solely by topographic acceleration of airflow (e.g. Gares and Nordstrom, 1995; Whitney *et al.*, 2015). Small depressions in a dune crest can channelize, compress and hence accelerate the air flowing through them. This results in an increased erosion rate (Carter, 1988). The depression will subsequently increase in size to develop into a full-scale blowout.

(3) Climate change may increase the likelihood of blowout formation in two ways. A prolonged dry period may reduce the protective vegetation cover and thus allow for the formation of blowouts by wind erosion (Thom *et al.*, 1994). Alternatively, an increase in average wind speed may also lead to the development of blowouts (Hesp, 2002; Hugenholtz and Wolfe, 2006).

(4) Local variations in vegetation cover and species due to e.g. nutrient availability, aridity or animal activity may lead to the subsequent development of blowouts by wind erosion (Jungerius *et al.*, 1981; Hesp, 2002).

(5) Rills, gullies and small debris fans that form on the slope of a dune after a rainfall event may reduce vegetation cover and accelerate air flowing through these features. Hence, water erosion may contribute to the development of a blowout, although Hesp (2002) concluded that these processes are only of minor importance.

(6) During strong winds, vegetation can be removed by undercutting. Blowouts can form on the bare surface that remains (Bird, 1974). Alternatively, wind-blown sediment may completely bury pre-existing vegetation, forming a new, bare surface on which a blowout may develop (Marta, 1958).

(7) Humans may contribute to the formation of trough blowouts by removing vegetation through trampling, forest felling, 4WD activity, constructions works, sand extraction, military training and fires (Hesp, 2002).

2.3. Foredune flow dynamics

In order to understand the flow dynamics in and around trough blowouts, it is important to address flow dynamics of the foredunes since many concepts apply to trough blowouts as well. Furthermore, the foredunes may also influence flow dynamics within trough blowouts that cut through a foredune ridge (e.g. Hesp and Pringle, 2001).

Numerous studies have shown that wind approaching a transverse or reversing dune crest obliquely, is realigned to a more normal flow direction over the crest (Arens *et al.*, 1995; Walker *et al.*, 2006; Jackson *et al.*, 2011; Pease and Gares, 2013; Smyth *et al.*, 2013). Besides the height and morphology of a dune, the angle of incidence is also an important factor in determining the degree of acceleration, topographical steering and secondary flow patterns of near-surface wind. Walker *et al.* (2006) described how incident oblique alongshore winds are deflected to more normal to the dune crest on the lower stoss slope, and are then deflected back to the original approach angle on the upper stoss slope. Maximum topographical steering of airflow occurs at oblique approach angles of 30° - 60° (Arens *et al.*, 1995). Arens *et al.* (1995) concluded that maximum acceleration of airflow occurs on the upper stoss slope of a foredune when on-shore winds approach it perpendicularly. At increasingly oblique angles, flow acceleration decreases until no flow acceleration occurs if the wind blows parallel to the foredune crest. On the lower stoss slope (and dune toe) airflow is often decelerated due to flow stagnation and surface roughness due to vegetation (Arens *et al.*, 1995; Walker and Nickling, 2002; Walker

et al., 2006). The effects of acceleration and deceleration increase with increasing dune height (Arens *et al.*, 1995; Parsons *et al.*, 2004). In addition, secondary flow patterns may develop. Secondary lee-side flow patterns include flow separation, which creates a highly-complex turbulent wake zone on the leeward slope including e.g. reversal cells, shear layers and internal boundary layers (Walker and Nickling, 2002). The presence and characteristics of these flow patterns are mainly governed by the wind approach angle (Jackson *et al.*, 2011; Lynch *et al.*, 2011) and dune morphology (Baddock *et al.*, 2011).

2.4. Primary flow dynamics

Trough blowouts that cut through a linear dune ridge modify the topography of a coastal dune area and hence they alter airflow patterns, erosion, and transportation of sediment in and around the blowout (Gares and Nordstrom, 1995; Fraser, 1998; Pease and Gares, 2013). Similar to transverse dunes, the general concepts of flow acceleration, topographical steering and the development of secondary flow patterns apply to trough blowouts. However, their characteristics are different in terms of magnitude, flow dynamics, approach angle threshold and form-flow relation.

The direction of on-shore winds that approach the trough blowout parallel to the blowout axis remains relatively unhampered upon passing through the blowout entrance and the deflation basin. Airflow is compressed and accelerated after passing through the blowout entrance (Figure 2a), forming a single, pronounced jet along the central blowout axis and several smaller jets along the erosional walls (Hesp and Hyde, 1996; Hesp, 1996). Upon leaving the blowout throat, the flow subsequently expands laterally over the transportational ramp and therefore decelerates, especially near the margins of the laterally expanding flow. However, along the center axis up the ramp, airflow accelerates again as it approaches the lobe's crest (figure 3, 4 and 13 in Hesp and Hyde, 1996; Fraser *et al.*, 1998). Downwind of the depositional lobe crest, flow separation occurs similar to transverse dunes (Hesp and Hyde, 1996; Hesp, 1996). Both flow acceleration over the depositional lobe crest and formation of downwind secondary flow patterns is comparable to transverse dunes, with the notable exception of the laterally expanding, decelerating flow found on a blowout's transportational ramp.

If on-shore winds approach the blowout axis at an oblique angle, a significant amount of topographical steering takes place (Hesp and Hyde, 1996; Hesp, 1996; Hesp and Pringle, 2001; Hesp, 2002; Pease and Gares, 2013; Smyth *et al.*, 2014). The airflow in the blowout entrance is deflected of the downwind erosional wall and thus becomes more aligned with the blowout axis (Hesp and Hyde, 1996; Pease and Gares, 2013). Obliquely approaching winds are 'sucked' into the trough blowout by a low pressure zone over the deflation basin (Hesp and Pringle, 2001; Hesp, 2002). In this way, winds approaching the blowout at an angle of up to 100° from the blowout axis can be steered

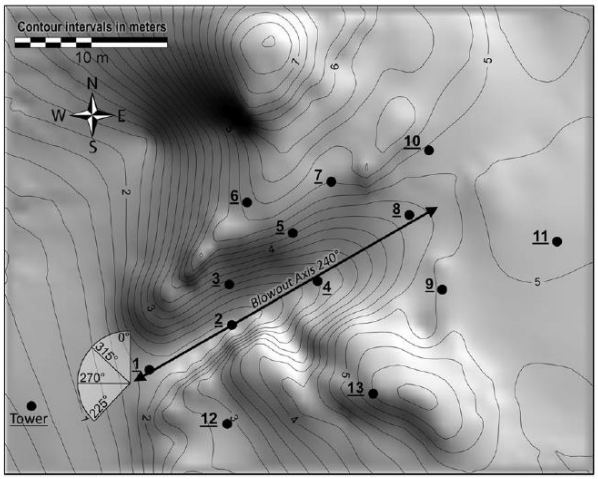

Figure 3. Measuring stations located in the trough blowout in the study of Pease and Gares (2013). (Source: Pease and Gares, 2013, pp. 1162

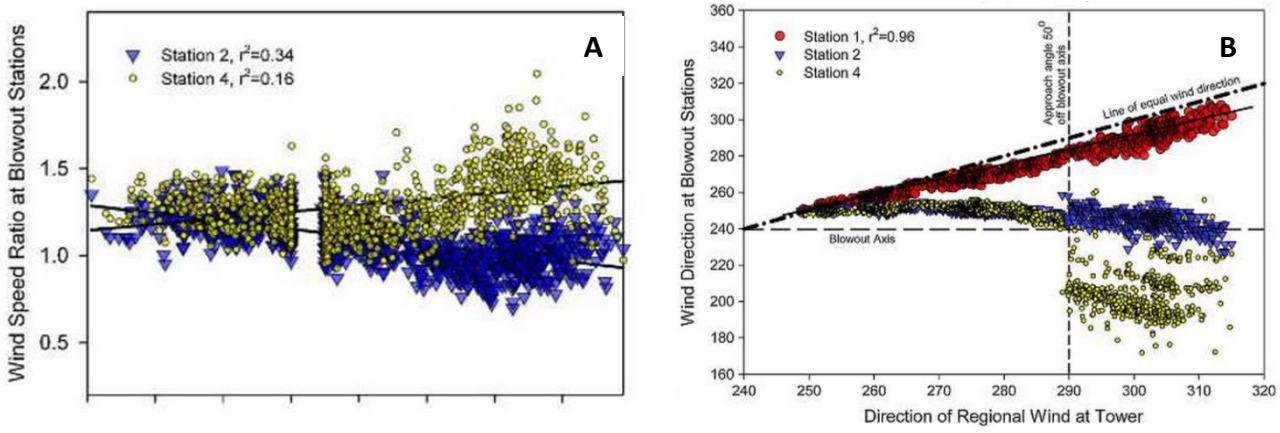

Figure 2. (A) Flow velocity at trough locations with respect to ambient wind speed; (B) Flow direction with respect to ambient wind direction. At station 1 (see Figure 3) wind direction has not yet been altered. At station 2 flow becomes aligned with the blowout axis and flow velocities are generally higher than ambient wind speed. Further down in the trough at location 4, close to the transportational ramp, flow is further accelerated. The sudden variability of flow direction at approach angles greater than 50° is possibly due to secondary flow. (Source: Pease and Gares, 2013, pp. 1164)

parallel to its center axis (Hesp and Pringle, 2001). Pease and Gares (2013) and Smyth *et al.*, (2014) found that winds approaching the blowout at angles of less than 50° are dominated by topographical steering, making flow patterns within the blowout independent of approaching wind angles within this range (Figure 2b andFigure **4**a). If wind approaches from oblique angles greater than 50°, the flow is no longer dominantly aligned with the blowout axis (Figure 2b andFigure **4**b). Instead, flow separation takes place over the rim dunes and secondary flow patterns form inside the trough (Pease and Gares, 2013; Smyth *et al.*, 2014).

The findings of Pease and Gares (2013) differ considerably from the 100° deflection angle suggested by Hesp and Pringle (2001). Pease and Gares (2013) attribute this difference to minor morphological differences, such as the sharper dune ridgeline, which may have facilitated flow separation over the crest earlier on. In addition, they recognize that topographical steering still takes place in the lower portion of the trough under higher approach angles, albeit the resulting axis-parallel jet flow is no longer dominant over secondary flow (Figure 4b).

During oblique on-shore directed winds, wind direction at the blowout entrance still matches the ambient wind direction (Pease and Gares, 2013). However, Hesp and Pringle (2001) suggested that low

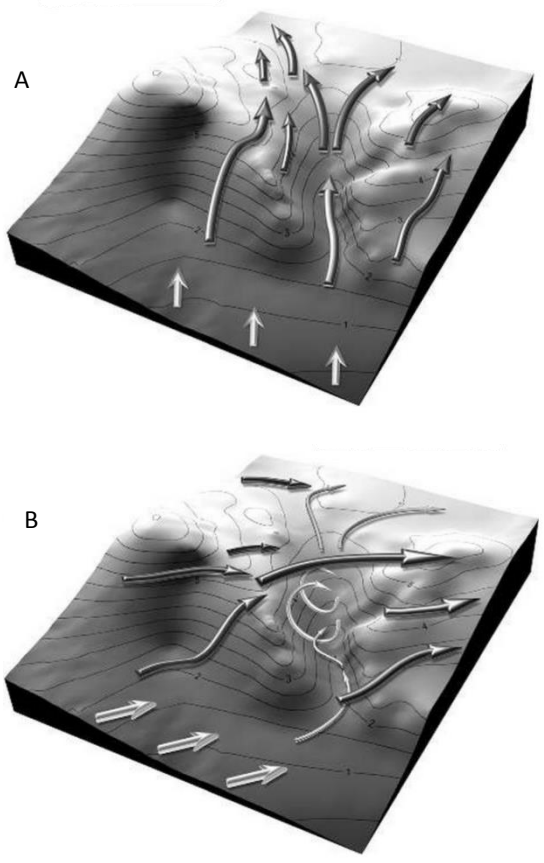

Figure 4. Flow patterns inside and around the trough blowout. (A) Wind approach angle < 50 ° (B) Approach angle > 50 °. Flow separating over the rim is clearly dominant over jet formation inside the trough at high approach angles (Source: Pease and Gares, 2013, pp. 1167-1168)

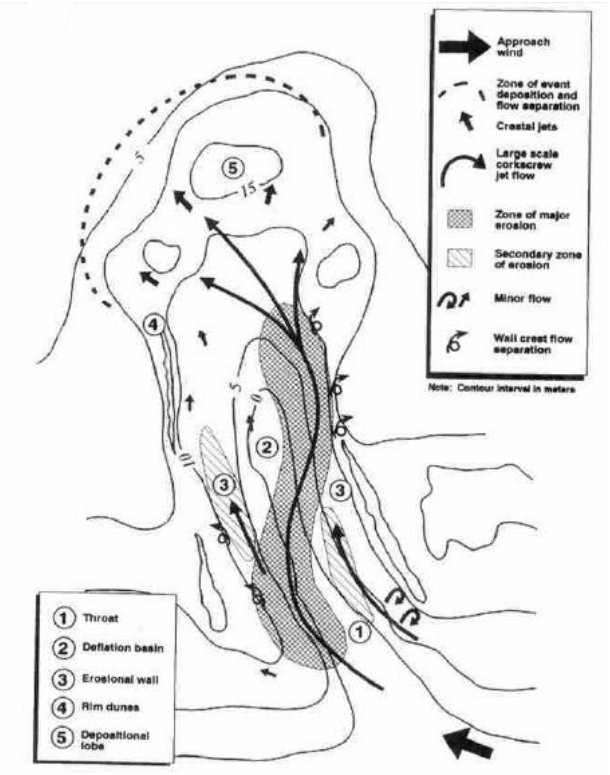

Figure 5. S-shaped flow inside the trough during oblique on-shore wind conditions. (Source: Hesp and Hyde, 1996, pp. 521.)

to moderately oblique flow may already be topographically steered to some extent by adjacent foredunes before reaching the blowout entrance. Upon contact with the erosional sidewalls, airflow is reflected towards the opposite sidewall. As a result, the path of the main jet within the blowout describes an S-shaped motion (Figure 5) (Hesp and Hyde, 1996; Pease and Gares, 2013). Similar to a situation in which winds approach parallel to the blowout axis, the airflow is compressed and accelerates in the central part of the blowout. Due to the S-shaped flow pattern, variations in flow velocity and direction may be observed, especially along the sidewalls. For example: in their N-S oriented trough blowout, Hesp and Hyde (1996) observed that flow velocity was greatest on the western sidewall, close to the depositional lobe. The SW approaching wind was first reflected off the eastern sidewall, close to the blowout entrance. Further down the trough, airflow accelerated along the western sidewall and subsequently separated over the sidewall and the adjacent depositional lobe. Pease and Gares (2013) found additional evidence for the S-shaped flow pattern within the trough. As wind approach angle shifted clockwise, local wind direction at the upwind-located sidewall (station 5, see Figure 3) shifted counter-clockwise. The inverse direction relationship confirms the existence of an S-shaped jet flow and supports the idea of the sidewall's reflective properties.

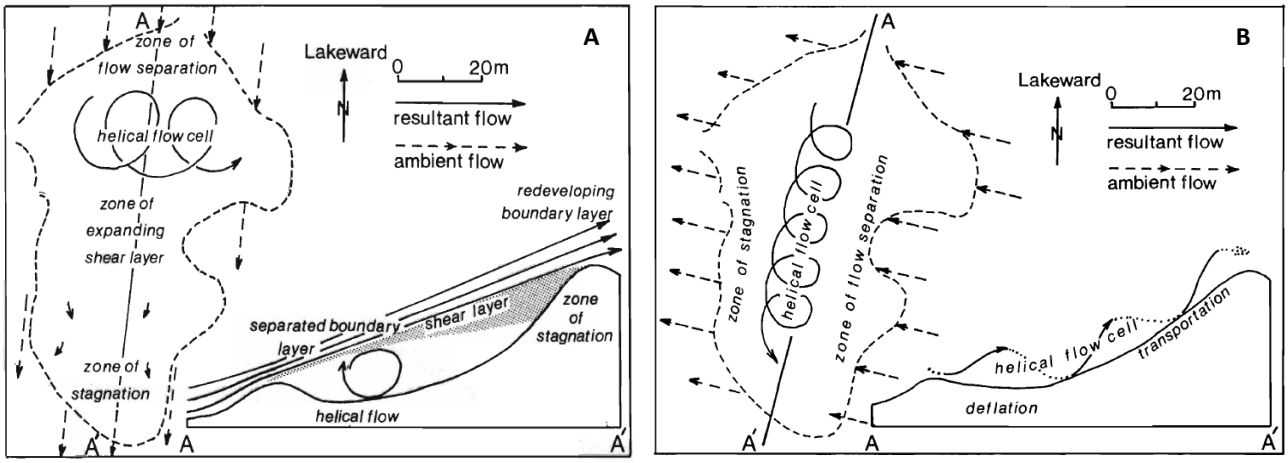

Figure 6. (A) Flow seperates at the entrance, forming an axis-parallel helicoidal flow inside the trough. (B) At higher approach angles, flow separation over the rim causes helicodal flow along the center axis. (Source: Fraser *et al.*, 1998, pp. 458-459)

2.5. Secondary flow dynamics

A number of secondary flow patterns may develop inside and around a trough blowout, especially if the wind approaches the blowout at oblique angles. Secondary flow patterns include (1) Helicoidal flow around the main jet (Fraser *et al.*, 1998; Hesp and Pringle, 2001; Pease and Gares, 2013); (2) Topographical steering of flow up the sidewalls and subsequent separation over the rim (Hesp and Pringle, 2001; Smyth *et al.*, 2014); (3) roller vortices on the lee side of rim dunes (Hesp and Hyde, 1996) and (4) Flow separation over the depositional lobe, causing lee-side secondary flow patterns similar to those for transverse dunes (Hesp and Hyde, 1996; Hesp, 1996).

The existence of helicoidal or corkscrew vortices within a trough blowout was first suggested by Hesp (1996) and Hesp and Hyde (1996). Winds approaching the trough blowout parallel to its axis may separate at the entrance (if deflation basin elevation is significantly lower), forming a helicoidal flow pattern oriented parallel to the blowout axis (Figure 6a) Oblique alongshore wind approaching the sidewall of a trough blowout separates over the rim, into the trough. This may results in a helicoidal flow around the main axis-parallel jet below the separated flow (Figure 6b and Figure **4**b, see also Hesp and Pringle, 2001). Pease and Gares (2013) also attribute some of the variability in wind speed and direction in the blowout to helicoidal flow. They found that, especially at approach angles greater than 50°, helicoidal flow dominated inside the trough (Figure 4b).

Airflow may also leave the trough by moving up the sidewall and separate over the rim (Hesp and Pringle, 2001; Hesp, 2002; Smyth *et al.*, 2014), resulting in the roller vortices on the lee side of the rim dune that were first observed by Hesp and Hyde (1996). Airflow originating from inside the trough blowout may be steered perpendicular to the erosional wall, in a similar way as airflow is steered onto the stoss face of transverse dunes (Smyth *et al.*, 2014). Due to the additional topographical steering onto the windward erosional wall, in combination with the inverse direction relationship found by Pease and Gares (2013), wind direction may completely reverse. If this is the case, airflow separating over the windward rim will meet ambient wind head on, possibly creating a large helicoidal roller vortice above the respective erosional wall (Hesp and Pringle, 2001).

2.6. Sediment transport

Trough blowouts are important pathways of sediment transport in a dune area (Byrne, 1997). A trough blowout features erosion, deposition and transfer of sediment. Due to flow dynamics inside trough blowouts, sediment transport estimates based on ambient wind may be up to two magnitudes lower than actual transport within the blowout (Hesp and Hyde, 1996).

Erosion typically takes place in several locations within the blowout. The most important sediment source is the deflation basin, which continues to erode until constricted by ground water level or a hard, unerodable surface (Hesp, 2002). Furthermore, the sidewalls play a role in sediment supply and transport in two ways. Slumping may occur on the poorly vegetated sidewall due to e.g. lowering of the deflation basin (see 'slump blocks' in Figure 1). Wasted material in the slump toe is subsequently removed from the deflation basin (Gares, 1992; Hesp and Hyde, 1996; Hesp, 2002). In addition, topographically steered and accelerated flow over the sidewall crest facilitates transport of sediment originating from the deflation basin and/or sidewall itself (Smyth *et al.*, 2014). Finally, erosion may occur at the crest of the depositional lobe, where winds are accelerated (Byrne, 1997). Besides sediment supply from within the blowout, beach sediment is commonly transported landward through the blowout to the foredune plain by on-shore winds (Gares and Nordstrom, 1995; Byrne, 1997; Anderson and Walker, 2006).

Sediment is typically deposited on the depositional lobe and on the rims (Hesp and Hyde; 1996; Hesp, 1996; Neal and Roberts, 2001; Hesp, 2002). Directly leeward of the depositional lobe crest, the flow separates and decelerates. Sediment is deposited on the lee-side of the depositional lobe through grainfall and sorting will take place as fine sediment is transported further downwind (Hesp, 1996; Hesp and Hyde, 1996). Deposition on this side of the lobe is also related to vegetation roughness, which decelerates the airflow (Anderson and Walker, 2006). Airflow along the central axis of the transportational ramp is stronger and is thus more often above the threshold of motion. Hence, most sediment is deposited on the central part of the depositional lobe, whereas away from the center axis sedimentation rate becomes gradually lower. Due to lateral spreading on the transportational ramp, sediment is more likely to deposit near its margins (i.e. on the windward slope of the depositional lobe). The latter processes are responsible for the parabolic shape of the depositional lobe (Hesp and Hyde, 1996, Hesp, 2002).

Sediment can be transported from within the blowout up the sidewalls and over the rim (Carter *et al.*, 1990; Fraser *et al.*, 1998; Hesp, 2002). This leads to the formation of rim dunes that are created below the separated flow that leaves the trough blowout (Carter *et al.*, 1990). Simultaneous lowering of the deflation floor leads to rapid (partially relative due to rim dune growth) deepening of the trough blowout. Spillover lobes are created under the flow that separates over the rim. They may either overtop the rim dune or create a shallow trough blowout cutting through the rim dune (Fraser *et al.*, 1998).

Sediment flux within a blowout is typically highly variable and difficult to correlate with primary or secondary flow patterns (Smyth *et al.*, 2014). In addition, flow dynamics may vary dramatically as a result from seemingly insignificant morphological differences (Pease and Gares, 2013). Besides morphological differences, variability in wind speed and direction further complicates the prediction of sediment transport patterns. In their study, Pease and Gares (2013) concluded that at approach angles of 50° or lower, the form-flow relation is determined by primary flow that is steered into the blowout. At angles greater than 50°, the form-flow relation is determined by secondary helicoidal flow. In a similar fashion, the form-flow relation can be dominated by a prevalent wind direction. Hesp and Hyde (1996) and Byrne (1997) noted that the regular occurrence of an obliquely approaching wind led to preferential erosion of one sidewall, causing the skewed orientation of the blowout and an asymmetrically-shaped depositional lobe. The latter process may also create lateral erosional lobes that extend outward from the deflation basin (Fraser *et al.*, 1998). Variation in vegetation cover is an additional factor that complicates sediment transport both spatially and temporarily. In a blowout at Pinery National Park, Canada, deposition mainly occurred in late-summer, whereas erosion was dominant throughout the winter (Byrne, 1997). In general, most sediment is transported in wet, cold and windy seasons.

2.7. Trough blowout dimensions

Few studies have been carried out that give a detailed overview of trough blowout dimensions during various stages of their development. Trough blowouts generally have a length-width ratio of 2:1 to 3:1 (Personal observation; also see examples in Hesp and Hyde, 1996; Fraser *et al.*, 1998; Hesp, 2002). Higher length-width ratios up to 10:1 may sometimes occur in certain areas (e.g. Myall Lakes Nat. Park, Australia; Manawatu-Wanganui coast, NZ). In absolute terms, the active part of a trough blowout can be anywhere between 10 m and 500 m long, with width varying according to the given ratios. The variability in trough blowout dimensions most likely relates to the environment (e.g. wave erosion; wind direction, speed and variability; moisture, nutrient availability and associated vegetation patterns; sand availability) and morphological conditions (e.g. foredune morphology; presence of embryo dunes). However, no detailed research has been carried out yet that specifically addresses trough blowout dimensions and the variability therein.

Hesp (2002) is one of the few authors that compared the dimensions of multiple trough blowouts. He compared deflation basin length, depth and width against the length of the depositional lobe (including transportational ramp) of a series of trough blowouts on the Manawatu-Wanganui coast, NZ. It appears that deflation basin length correlates moderately strong with depositional lobe length in an almost 1:1 ratio (Figure 7). Hesp (2002) speculates that this shows an evolutionary trend. As sediment is eroded from within

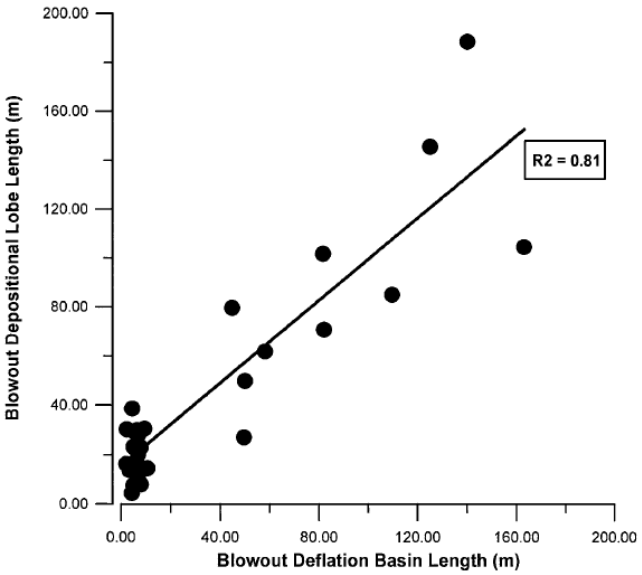

Figure 7. Depositional lobe length corresponds moderately strong with deflation basin length in a 1:1 ratio. (Source: Hesp, 2002, pp. 261)

the blowout, it is deposited on the leeward side of the depositional lobe, thus causing the lobe to expand somewhat proportional to the deflation floor. Depositional lobe length also correlates moderately strong with deflation basin width in a 1:2 to 1:4 ratio (Figure 8). Although no direct comparison of deflation basin width and length was made by Hesp (2002), the two relations are in line with an average length-width ratio of 2:1 to 3:1.

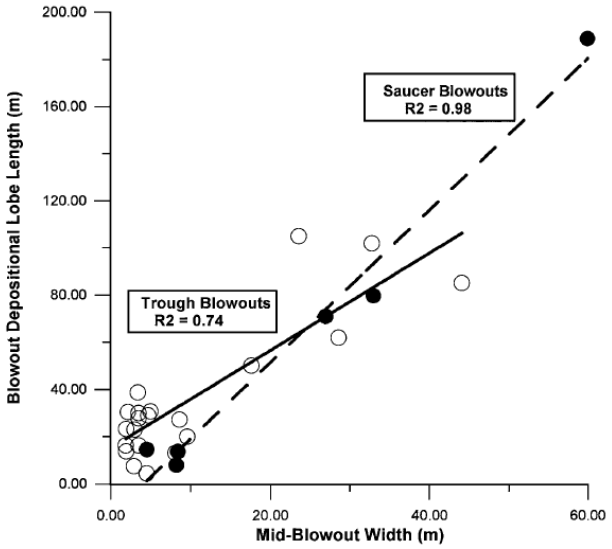

Figure 8. Depositional lobe length also correlates moderately strong with mid-blowout width, especially in the case of saucer blowouts. (Source: Hesp, 2002, pp. 261)

2.8. Blowout evolution

The formation and evolution of a blowout is a decadal-scale process (Dech *et al.*, 2004; González-Villanueva *et al.*, 2011). Once the conditions for blowout development have been set, its further evolution is determined by the interaction between aeolian processes, morphology and vegetation (Hesp, 2002; González-Villanueva *et al.*, 2011).

A trough blowout expands both laterally and vertically. The sidewalls retreat if the slope becomes oversteepened and slumping occurs (Carter *et al.*, 1990; Gares, 1992). The depositional lobe migrates away from the deflation basin and thereby enhances its length. In addition, the deflation floor is lowered due to erosion until a certain base level is reached, such as the seasonally lowest water table, a hard layer, or an armoured surface (Hesp, 2002).

A trough blowout can be deactivated to become an incipient blowout. There are two main causes for blowout deactivation: (1) Overgrowth, (2) revegetation, and (3) blocking by embryo dunes. Due to continued growth, the blowout may become too wide for the creation of jet flow, which decreases the blowout's ability to transport sediment (Hesp, 2002). Revegetation of the sidewalls and the deflation basin may lead to deactivation of the blowout (Gares and Nordstrom, 1995; Dech *et al.*, 2004). Revegetation on a decadal scale is a result of natural processes of retrogression and colonization (Dech *et al.*, 2004) and/or dune stabilization activities (Gares and Nordstrom, 1995). Finally, embryo dune development across the blowout mouth may block the entrance and deactivate jet flows inside the trough (Hesp, 2002; Battiau-Queney, 2014).

It is common for the depositional lobe to develop into a parabolic dune (e.g. Carter *et al.*, 1990; Byrne, 1997, Hesp, 2002, Arens *et al.*, 2013), as the depositional lobe already develops a parabolic shape while the trough blowout is still active (Hesp and Hyde, 1996; Hesp, 2002). Hence, deactivation of the blowout allows the depositional lobe to continue to develop as a parabolic dune. Hesp (2002) suggested that this transformation typically concurs with the formation of embryo dunes on high energy wind coasts. If the embryo dunes blocking the entrance are removed by e.g. wave erosion, the blowout can be reactivated.

3. Methodology

3.1. Study site

The study area is located on the approximately N-S oriented Dutch coast roughly 6 km west of Bloemendaal (Figure 9) and is part of Zuid-Kennemerland National Park. The five trenches were created in the 2012-2013 winter season and are located on a 700 m stretch of foredune. The foredune

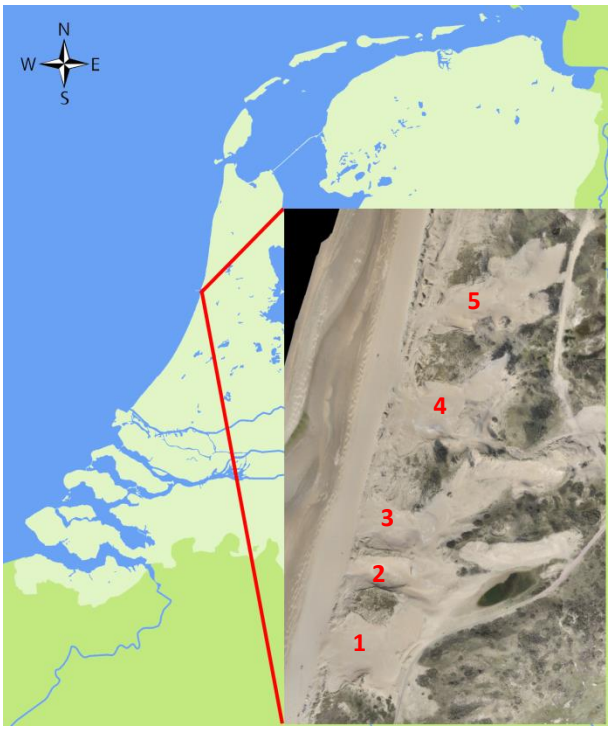

Figure 9. Location of the study site. Aerial photograph of the study site was taken on 21-04-2015. Numbers indicate trenches, and will be used to refer to a trench in this report.

ridge reaches heights of up to 20 m above the mean sea level and is 150-200 m wide. The trenches were

Figure 11. Dune valley at Zuid-Kennemerland. Picture was taken from the foredune ridge. Damp dune valleys are located behind the foredunes and may feature swamps and small pools. Large scale parabolic dunes are visible on the right side of the picture. The skyline of Ijmuiden can be seen on the horizon.

dug down to a level of 6 m +NAP (Dutch Ordnance Datum) (Kuipers, 2014). Trench 1 currently provides public access to the beach. Therefore it is actively maintained in order to make sure that the bicycle storage and bicycle path behind the trench do not get covered by sand. Sand removed from behind the trench is frequently relocated to the beach or just in front of the trench. Behind the foredune ridge there typically is a damp dune valley and an associated inactive parabolic dune. Some damp dune valleys feature swamps or small pools (Figure 11). A complex system of (inactive) parabolic dunes is located further landward (Arens *et al.*, 2004). The entire dune system in Zuid-Kennemerland National Park is about 3 to 4 km wide.

The climate on the Dutch coast is temperate and is characterized by strong seasonal contrast (Arens *et al.*, 2013). In the period between April 2014 and April 2015, precipitation amounted to a total of 900 mm during a total of 615 hours. Late-summer precipitation in the Dutch coastal provinces is generally stronger than further inland (KNMI, 2008). Wind generally comes from the west to southwest, with strongest winds coming from the southwest during late-autumn and winter. A detailed overview of wind rose data is given in Figure 10.

3.2. DEM creation and analysis

Data for the Digital Elevation Models (DEMs) were collected during the period between April 2014 and April 2015. A total of four DEMs, A through D, were made based on measurements conducted in this period. Data for the DEMs was retrieved by flying over the study area with an Unmanned Aerial Vehicle (UAV). Around 1000 – 1500 aerial photographs were taken during several flights on a single day. The photos were processed with Agisoft Professional following the same procedures as Javernick *et al.* (2014) in their study. Agisoft tracks a selection of unique pixel-based features and matches these between multiple aerial photographs. Combined with orientation parameters, a sparse point cloud is generated (containing elevation data) and the location and position is determined for all images. A dense point cloud (every pixel) is subsequently created from pixels on the image and the

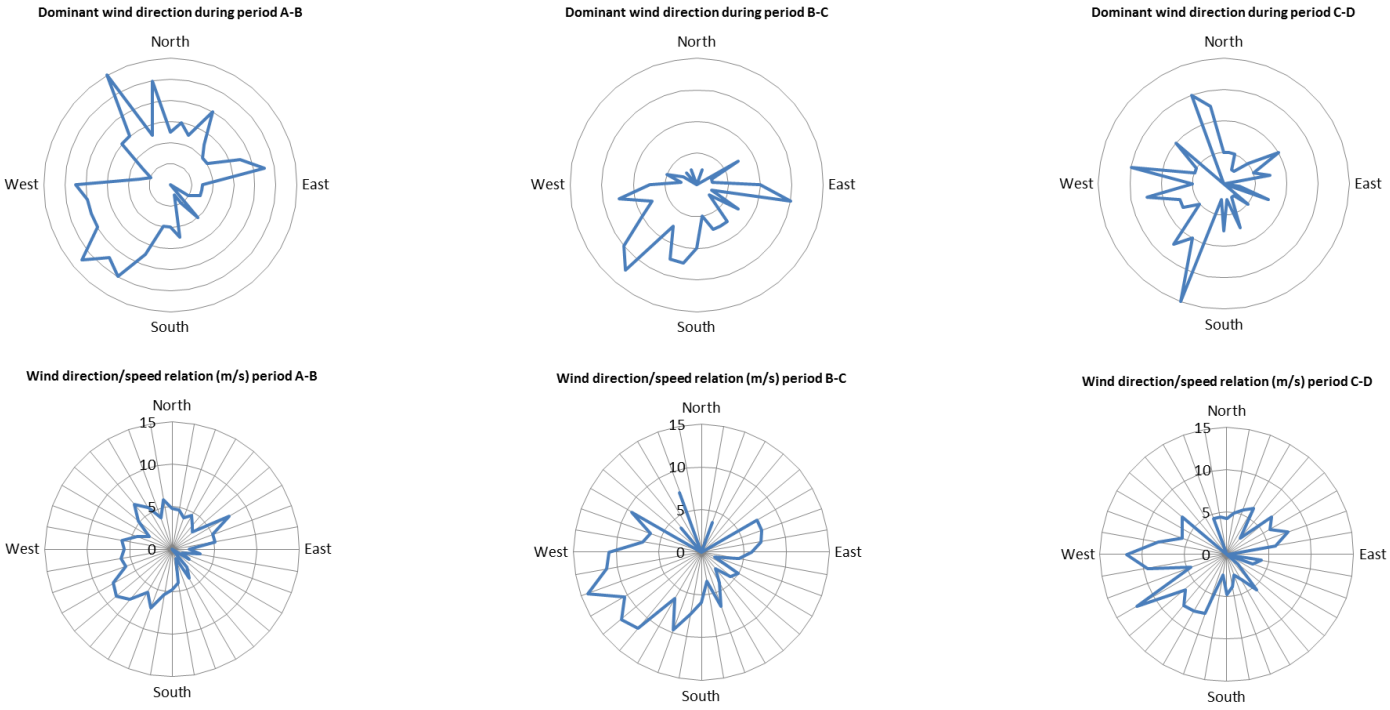

Figure 10. Wind rose data. Period A-B: 10-04-2014 – 27-10-2014; period B-C: 28-10-2014 – 18-01-2015; period C-D: 19-01-2015 – 21-04-2015. Dominant wind direction indicates relative occurrence of wind coming from a certain direction. Data was retrieved from Ijmuiden and provided by the Royal Dutch Meteorological Office.

determined camera orientations and locations. The dense point cloud is located in an arbitrary coordinate system, but can be placed in a geographical coordinate system through the use of Ground Control Points (GCPs). A total of 40 GCPs were placed in the study area. The locations of these GCPs were determined in the field by GPS. The GCP's geographical location was then manually assigned to the respective GCP object in the aerial images. Based on the geographical locations of the GCPs, the arbitrary coordinate system was converted to Rijksdriehoekcoördinaten (Dutch coordinate system) by applying a linear transformation. A cell size of 1 m x 1 m was chosen for the DEMs. Points from the point cloud within the range of a grid cell were averaged to determine the z-coordinate (elevation) of the grid cell. Digital Elevation Models were exported to ESRI ASCII raster format. The raster of a DEM for the entire study area has 501 columns and 801 rows.

The DEMs were digitally analyzed using ESRI ArcGis ArcMap 10.2.2 and SAGA GIS 2.1.4. The following data were retrieved or visualized from the basic DEMs: (1) Difference maps; (2) slope maps; (3) classified polygon layers; (4) volume changes of classified features; (5) dimensions of individual features; (6) average deposition and erosion rates at various locations; and (7) long profiles and cross profiles.

Morphological changes were visualized in difference maps. Since all DEMs are represented by a 501 x 801 matrix, they can easily be subtracted from each other in order to create a difference map. The subtraction yields a 501 x 801 matrix, with each cell containing a positive or negative value representing elevation change (0 means no change). A total of three difference maps were created for each consecutive pair of DEMs (hereafter referred to as 'change map A-B, B-C or C-D' and time period A-B etc. to refer to the period between two DEMs). Volume and surface area differences can readily be observed from the difference maps. A slope map was automatically created for each individual DEM using the ArcGis 'Slope' spatial analyst tool.

Morphological features, such as a depositional lobe or erosional basin, were manually selected by drawing a polygon feature class covering the respective morphological feature in ArcMap. The selection is based on interpretation from the difference maps, slope maps and basic DEMs (Figure 14). A depositional lobe is selected based on shape, position and orientation with respect to the blowout axis, and deposition. The latter criterion means that the transportational ramp, crest or any other inactive parts are not included in the calculation as they are not predominantly areas of deposition, but rather erosion. Depositional lobe in this context should thus be referred to as 'active part of the depositional lobe', or 'active lobe' for short. The actual volume of the depositional lobe with respect to a certain base level is far greater, but not relevant for the purpose of this paper. A deflation basin is selected based on shape, position within the blowout area, bounding sidewalls indicated by the slope maps, and erosional pattern derived from the difference map. Finally, sidewalls were selected based on slope angle and active erosion. Furthermore, only the part of the sidewalls adjacent to the deflation basin has been selected in order to get consistent and comparable results. One classification was made for sidewalls and deflation basins to ensure comparable results. For the more dynamic active lobes, a total of three classifications were made based on each consecutive pair of DEMs.

The classified polygons containing the morphological features were isolated from the difference map and exported as individual raster. The amount of rows and columns of such a raster depends on the maximum lateral extent of the morphological feature. The cells of the matrix hold the same information as the difference map. The total volume below the raster surface can be calculated with the surface volume 3D analyst tool provided by ArcGis. Volume was calculated above a plane elevation of 0 for areas of deposition or below a plane elevation of 0 for areas subject to erosion. Volume below a plane elevation of 0 was subtracted from volume above the plane. This gives the net volume change, with negative values indicating net erosion and positives indicating net deposition. The calculated volume of the feature represents erosion or deposition over a given period of time (i.e. time between two consecutive measurements).

The surface areas of the morphological features are not equal and even through time an individual feature may vary in size (i.e. active lobes in this study). Thus, to provide an insight into relative depositional or

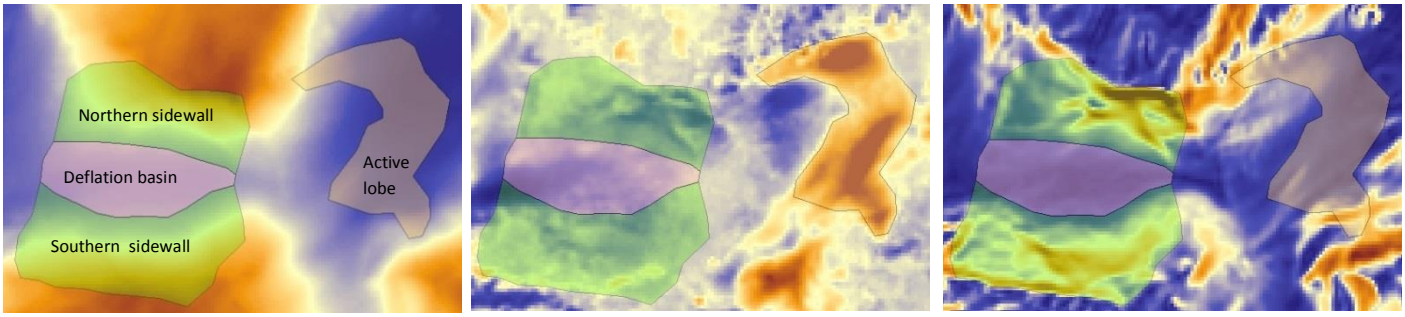

Figure 12. Example of the classified polygon layers projected on a basic DEM (left), difference map (middle) and slope map (right). Classification was done by interpretation based on these maps. A polygon is exported from the difference map in order to calculate volume change over the given period of time.

erosional activity, net volume change is normalized to surface area. This number represents the average elevation change over the entire feature. On the bare surface in the trough area, negative elevation change (lowering of surface) is associated with erosion; positive elevation change (raising of surface) is associated with deposition. Using averaged elevation change allows for easy comparison between similar morphological features in terms of erosion or deposition rate.

Dimensions of the deflation basins and active lobes were measured by creating a polyline feature class in ArcMap. The lines were fitted inside the deflation basin polygons to measure their length. Dominant length of the active lobe is determined by measuring down its central axis, which roughly divides the lobe in equal volumes parallel to the blowout axis. The dominant total width of the blowout is determined by the sum of the average northern wall width, average southern wall width, and average deflation basin width.

Cross and Long profiles were created using a combination of ArcGis and SAGA GIS. A new polyline feature class was created in ArcGis to determine the locations of the cross and long profiles. Cross profiles were placed in the central part of the deflation basin and perpendicular to the blowout axis. Long profiles were placed along the blowout axis, through the center of the deflation basin. The polyline feature class was then converted to a shapefile and projected on a DEM in SAGA. The SAGA tool 'profile from line' was used to create a new shapefile containing a series of points with an interval of 1 m along the profile line. The points take x, y and z information from the DEM that they are projected on. Thus, each point contains the elevation (value) of the underlying grid cell. The data was exported in tabular form to Microsoft Excel 2010 for the creation of graphical profiles.

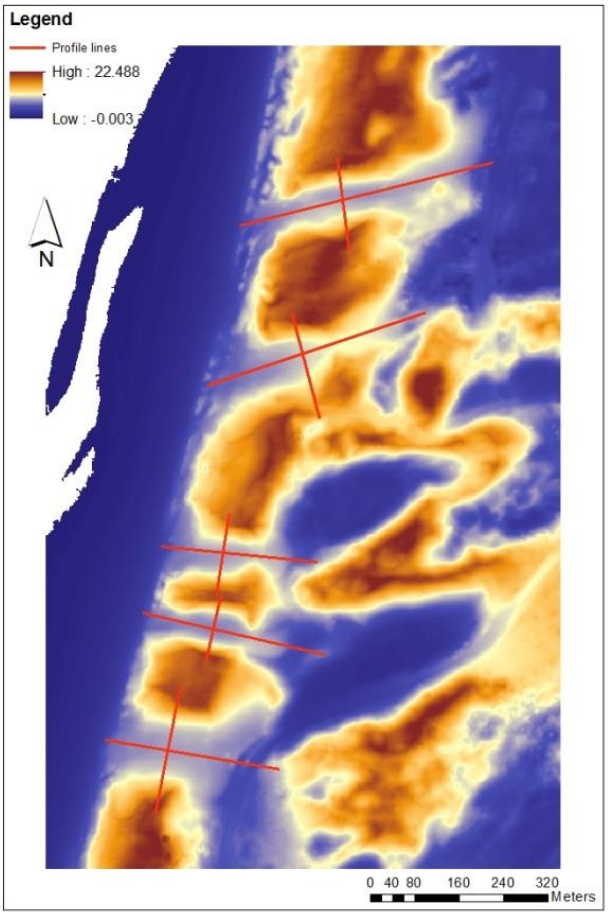

Figure 13. Location of the profile lines within the trenches.

4. Results

4.1. Shape and dimensions

From visual inspection of the DEMs it appears that the troughs have remained in their original position over the period of time between DEM A (April 2014) and DEM D (April 2015). The trough length to width ratio varies from around 1 to 1,6. There was no significant widening or elongation visible from the DEMs (Figure 14). Only the southern sidewall of trench started to retreat slightly during period C-D. Surface elevation within the blowout, sidewall slope angle and active lobe area volume and location have varied considerably (see change maps, Figure 15). All measured and calculated results are given in table 1.

All trenches are U-shaped across. The northern sidewall is typically steeper than the southern sidewall. All sidewalls slopes became up to 3° steeper during the one-year period between A and D (Figure 16,Figure 17 Figure 18). Along the blowout axis, the shape is more difficult to describe and different for each trench. For trenches 1, 2, 3 and 5, there is a ramp leading up from the backshore to the deflation basin, raising the surface by about 4-6 meters in about 40-70 meters distance (Figure 16,Figure 17 Figure 18). For trenches 1, 2 and 3, the ramp is followed by a small (0,5 m deep) depression, which coincides with the location of the deflation basin. Behind the depression, there is a relatively steep landward facing slope, dropping the surface by about 4-5 meters in about 20-40 meters distance (Figure 16 and Figure 17). Trench 5 is an exception as the depression does not (completely) coincide with the deflation basin, but is located further landward. The highest point in trench 5 is located in the middle of the deflation basin (Figure 18). Trench 4 is also an exception as the ramp leading up from the backshore continues all the way up to the point where the surface starts to drop again (Figure 17).

4.2. Deflation basins & blowout mouth

The deflation basins have been subject to both deposition of sediment and erosion. Deposition was common in or just in front of the blowout mouth (i.e. the seaward boundary of the deflation basin) (Figure 15). Strong deposition (100 – 200 m^3) took place in front of trench 1 and 5 during time period A-C. Depositional activity in front of these trenches seemed

to have decreased to only a few 10's m^3 sand in time period C-D. Sporadic areas of (minor) deposition inside the deflation basins were commonly activated and subsequently deactivated throughout the year. The deposited volume in the deflation basin was in the order of a few 10's m^3 in between DEM creation dates.

Erosion was dominant in all trenches throughout the entire year, with the exception of deflation basin 3 during time period A-B, which gained about 20 m^3 of deposited sand in the deflation basin. There is no general trend in erosion rate that can be observed from the data. On average, erosion rate was highest in time period B-C and lowest in time period C-D. In period A-B, erosion rates show much more variation between the different deflation basins. In time period B-D, erosion rates seem to have become more consistent with each other (Table 1). Deflation basin 1 lost the most sediment over the entire period of one year (1230 m^3, average erosion rate: 0,40 m/yr), followed by basin 2 (944 m^3, 1,02 m/yr), basin 5 (915 m^3, 0,55 m/yr), basin 4 (689 m^3, 0,47) and finally basin 3 (369 m^3, 0,49 m/yr). Surface lowering is also visible in the long profiles (Figure 16,Figure 17 Figure 18) and corresponds to the calculated erosion rates in Table 1.

There was a significant amount of erosion in deflation basin 2 in time period A-B. On average, the surface was lowered by 0,72 m, which is an order of magnitude greater than elevation change in the other deflation basins during the same period. Since the surface area of deflation basin 2 was relatively small, total volume loss from the deflation floor was more comparable to that of the other deflation basins. Still, the relatively small deflation basin lost a threefold of sediment compared to its much larger counterparts such as 1 and 4. The significant loss of sediment from deflation basin 2 in both absolute and relative terms was only observed for time period A-B. In time period B-D, surface elevation change was similar, or even slightly lower than in the other deflation basins.

4.3. Sidewalls

The sidewalls of the trenches have been predominantly areas of erosion. Similar to the deflation basins, localized areas of deposition may occur on the sidewalls. Areas of deposition are typically located either near the top or the bottom of the sidewall slope. Deposits are less common on the blowout rim.

The total amount of erosion from the sidewalls exceeded erosion from the adjacent deflation basin throughout the entire period A-D. The largest volume was removed from the sidewalls of trench 1 (2912 m^3, average erosion rate: 0,52 m/yr), followed by trench 5 (2555 m^3, 0,55 m/yr), trench 2 (2505 m^3, 0,96 m/yr), trench 4 (1760 m^3, 0,47 m/yr) and finally the least amount of material was removed from the sidewalls of trench 3 (1495 m^3, 0,49 m/yr). Especially during period A-B, sidewall erosion exceeded deflation basin erosion in trench 1 and 5 by a ratio of 8:1 and 13:1 respectively. During time period B-C, the significance of sidewall erosion with respect to deflation basin erosion decreased, but still remained dominant. Especially on the southern sidewalls, there were some depositional spots (Figure 15c), responsible for 10 - 150 m^3 of deposits depending on the location. Over the entire period of one year, the total eroded volume from the sidewalls was about 2,5 times greater than eroded volume from the deflation basin. In trench 3, this ratio is even greater at 4:1.

Although volume loss in a trench is mainly determined by its sidewalls, the average sidewall erosion rate is similar to erosion rate in the deflation basin. In general, erosion rate was greatest during time period A-B. Erosion rate was lowest during time period B-C, as opposed to erosion rate in the deflation basins, which was relatively high at that time. Variation in erosion rates between the trenches was greatest in time period A-B, but gradually decreased. From comparison of northern and southern sidewall erosion rate, it appears that in general, the southern sidewalls of trenches 2 and 5 had a significantly higher erosion rate during period A-B. On the other hand, trench 4 saw most of its erosion on the northern sidewall. Interestingly, all trenches saw mostly northern sidewall erosion during period B-C. Erosion was up to 5 times higher on the northern sidewall of trench 2 compared to its southern sidewall. In trench 4, the bias towards northern sidewall erosion increased further to about 8 times the southern sidewall erosion. In the period between C and D, erosion rate became more consistent between trenches (i.e. SD between trenches became lower, see Table 1), but erosion on the northern sidewall still dominated.

4.4. Depositional lobes

The active part of the depositional lobes has been the most active area both in terms of volume changes and migration rate. The surface area of all active lobes increased during the entire one-year period. In addition, the active lobes behind trenches 1, 3, 4 and 5 migrated in a northeastern direction. The active lobe behind trench 2 expanded and migrated towards the east. During period C-D, some previously abandoned areas of deposition closer to the deflation basin were reactivated, thus enhancing the size of the active lobe considerably. In the same period, the active lobe of trench 1 expanded so far north that it almost touches the active lobe of trench 2. Active lobes 1, 2, 3 and 5 are located in the dune valley behind the foredune ridge, whereas active lobe 4 is located inside the foredune ridge, constricting its lateral extent.

Deposition rate on the active lobes was very high at 1,6 to 2,8 m/yr compared to erosion rates inside the trough of only 0,3 to 1 m/yr. In the one-year period between A and D, deposits locally reached a thickness in excess of up to 5 meters (Trench 4, see Figure 17). Especially active lobes 2 and 4 saw an exceptionally high deposition rate in the period between A and C. Deposition rate shows a trend of steady decrease

towards the end of the measuring period. Similar to the deflation basins and sidewalls, variation in deposition rates between the active lobes decreased with time, indicated by the lower standard deviation. The total volume deposited in the active lobes exceeds the eroded volume from the sidewalls and deflation basin combined for trenches 1, 3, 4 and 5. Only for trench 2, eroded volume in the trough area exceeded the volume of deposits on the active lobe (Table 1).

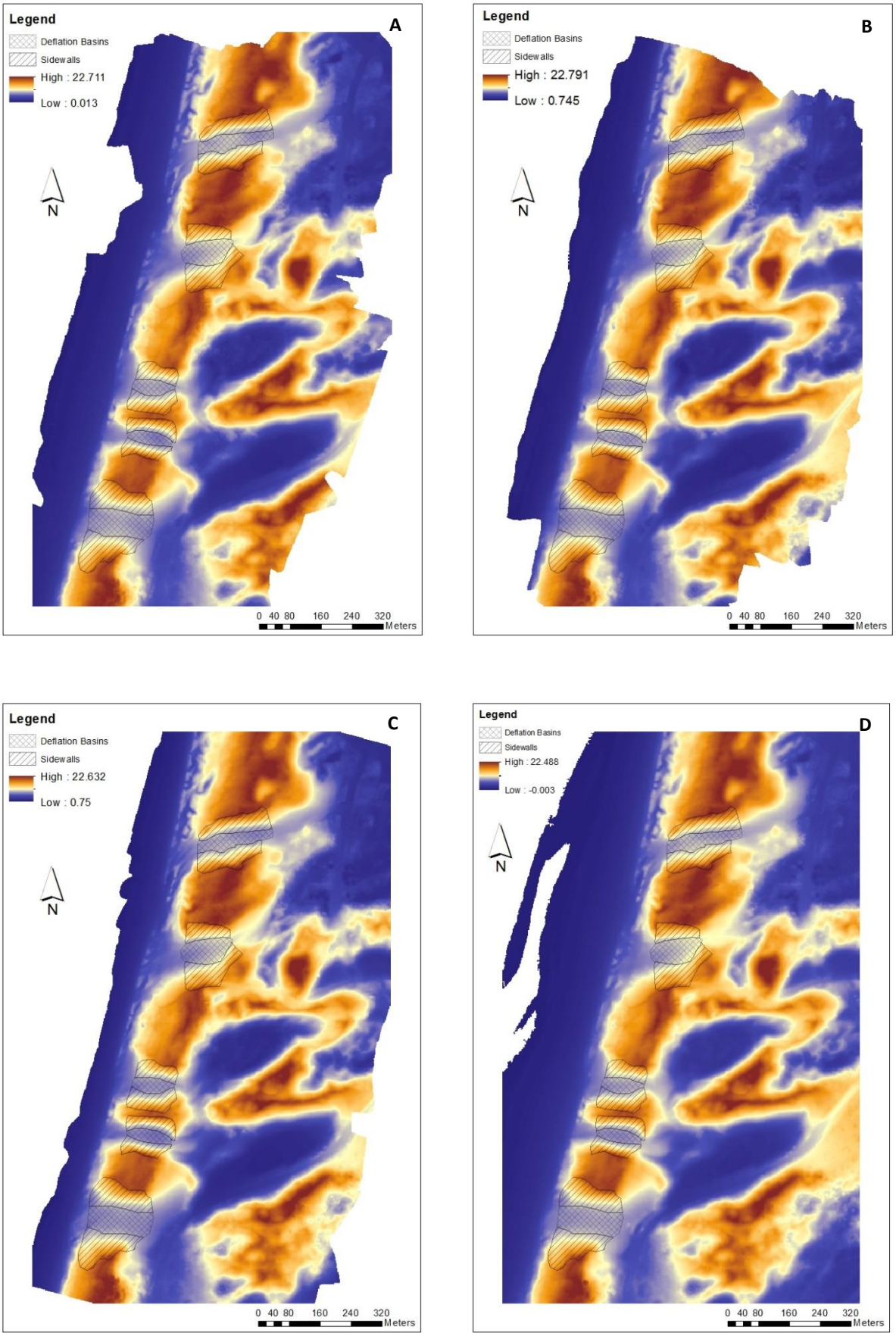

Figure 14. Digital elevation models. (A) 10-04-2014; (B) 28-10-2014; (C) 19-01-2015; and (D) 21-04-2015. Classified deflation basin and sidewall features are indicated. No obvious change in trough lateral dimensions is visible from the DEMs.

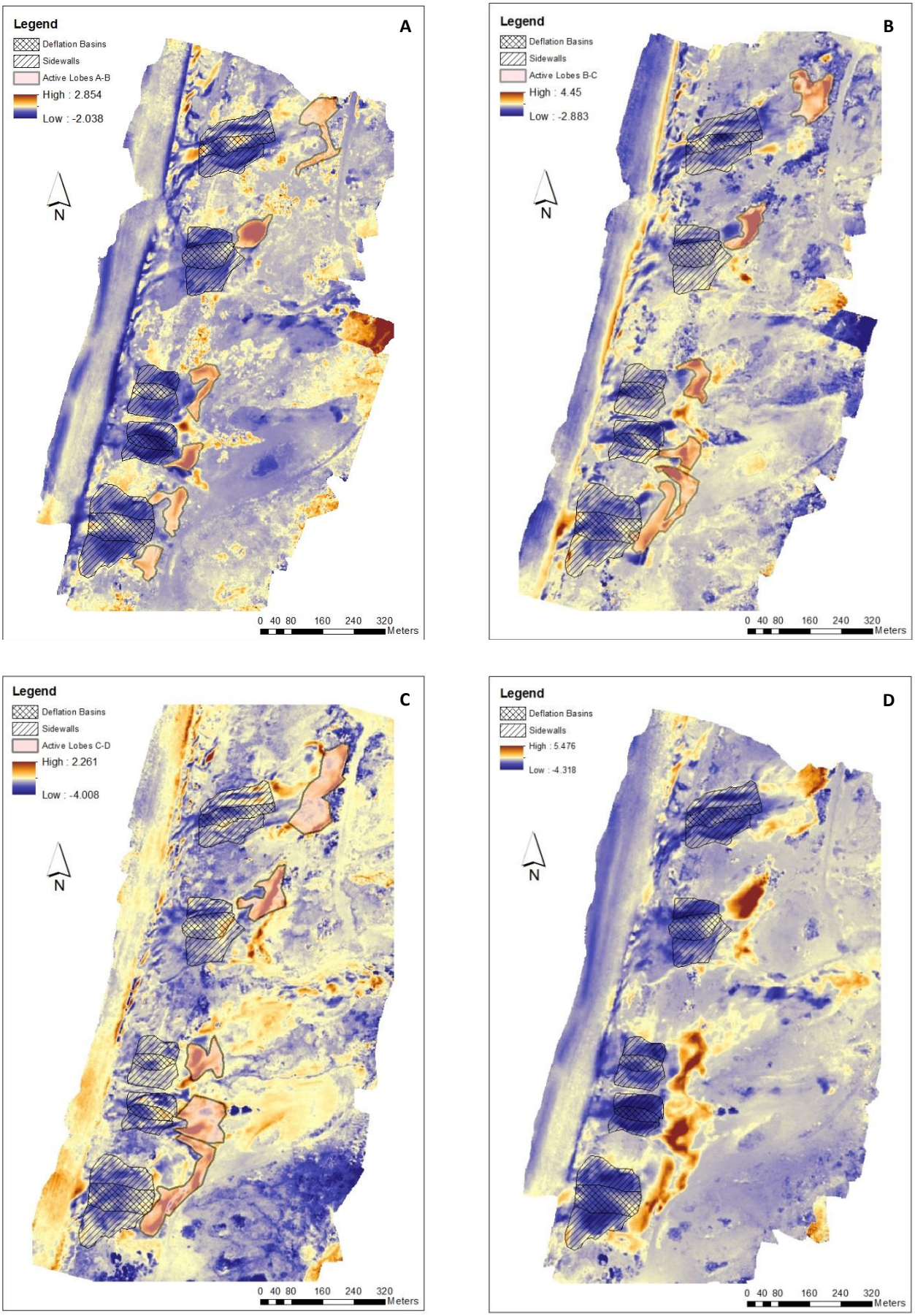

Figure 15. Change maps. (A) change map AB; (B) change map BC; (C) change map CD; and (D) 1-yr total change map. Areas of deposition and erosion can readily be observed from these maps. Classification polygons of active lobes cover areas of deposition behind the trenches. Note that the scale is different for each map (minimum value and maximum elevation).

Table 1. All measured and calculated data from the DEMs. DB = deflation basin; SW = sidewall; DL = depositional lobe. AB denotes the period between DEM A and B. For example: SWs net volume change CD means the volume change of the sidewalls over the period between DEM C and D. Positive values denote an increase in volume or elevation (deposition). Negative values indicate erosion. N-SW : S-SW is the ratio between northern sidewall erosion and southern sidewall erosion. A value greater than 1 implies northern sidewall preferential erosion and vice versa. DL excess sediment is defined by trench volume loss (SWs + DB) subtracted from DL volume gain. It indicates how much extra sediment is deposited on the depositional lobe that did not originate from the sidewalls or deflation basin.

Trench #	1	2	3	4	5	SD of row
Blowout length (m)	90	63	60	75	107	-
Blowout average width (m)	104	53	64	76	66	-
Blowout length/width ratio	0,86	1,17	0,93	0,98	1,62	-
DB polygon area (m^2)	3105	926	1020	2026	1881	-
South-SW polygon area (m^2)	2899	1215	1737	2423	2309	-
North-SW polygon area (m^2)	2752	1407	1297	1333	2359	-
DB net volume change AB (m^3)	-151	-619	20	-228	-82	-
DB net volume change BC (m^3)	-569	-217	-288	-313	-446	-
DB net volume change CD (m^3)	-510	-108	-101	-148	-387	-
DB total volume change (m^3)	-1230	-944	-369	-689	-915	-
DB average elevation change AB (m)	-0,05	-0,74	0,02	-0,12	-0,05	0,31093
DB average elevation change BC (m)	-0,19	-0,26	-0,31	-0,16	-0,26	0,057585
DB average elevation change CD (m)	-0,17	-0,13	-0,11	-0,08	-0,22	0,056621
DB average erosion rate (m/yr)	0,40	1,02	0,36	0,34	0,49	
SWs net volume change AB (m^3)	-1250	-1268	-842	-834	-1100	-
SWs net volume change BC (m^3)	-771	-686	-354	-360	-980	-
SWs net volume change CD (m^3)	-891	-551	-299	-566	-475	-
SWs total volume change (m^3)	-2912	-2505	-1495	-1760	-2555	-
SWs average elevation change AB (m)	-0,23	-0,53	-0,30	-0,24	-0,25	0,124538
SWs average elevation change BC (m)	-0,14	-0,29	-0,13	-0,10	-0,22	0,077299
SWs average elevation change CD (m)	-0,17	-0,23	-0,11	-0,16	-0,11	0,050489
SWs average erosion rate (m/yr)	0,52	0,96	0,49	0,47	0,55	
DL net volume change AB (m^3)	1470	1003	1109	1736	1276	-
DL net volume change BC (m^3)	1917	689	939	1632	1457	-
DL net volume change CD (m^3)	1583	874	730	895	918	-
DL total volume change (m^3)	4970	2566	2778	4263	3651	-
DL average elevation change AB (m)	0,58	1,11	0,83	1,31	0,59	0,322238
DL average elevation change BC (m)	0,54	0,58	0,73	1,14	0,58	0,250358
DL average elevation change CD (m)	0,46	0,34	0,40	0,45	0,25	0,087939
DL average deposition rate (m/yr)	1,60	2,77	2,72	2,10	1,94	
N-SW : S-SW av. el. change AB	0,86	0,55	1,24	1,70	0,45	-
N-SW : S-SW av. el. change BC	2,65	5,00	1,57	7,71	1,22	-
N-SW : S-SW av. el. change CD	1,32	1,04	1,97	1,82	0,52	-
DL 1-yr excess sediment (m^3)	828	-883	914	1814	181	-
SW : DB erosion ratio	2,37	2,65	4,05	2,55	2,79	-

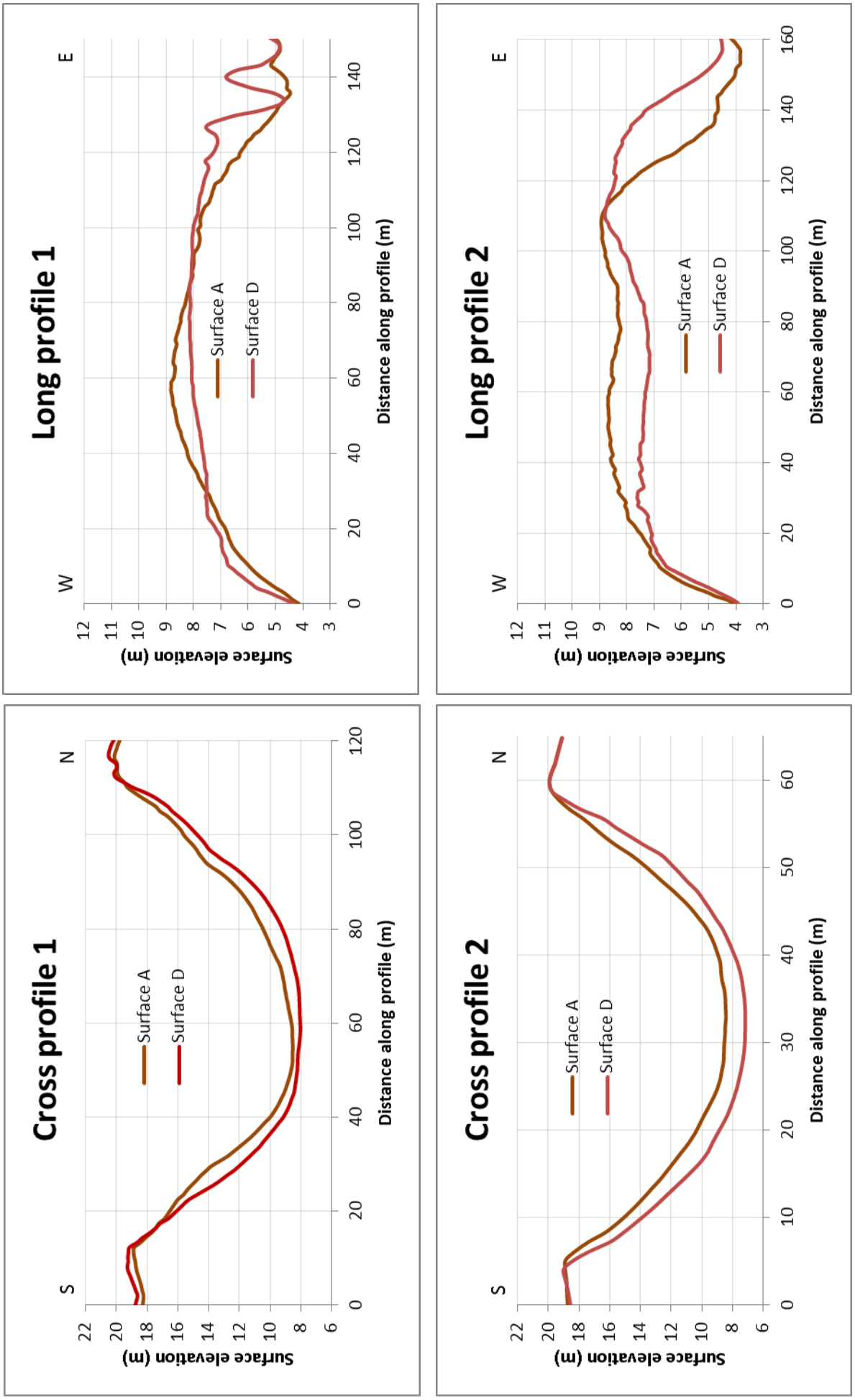

Figure 16. Cross and long profiles or trench 1 and 2. Sidewall evolution is very well visible in cross profile 2. The sidewall becomes steeper on average. Deflation basin depression is clearly visible in long profile 2. Also note the slight retreat of the southern sidewall of trench 2.

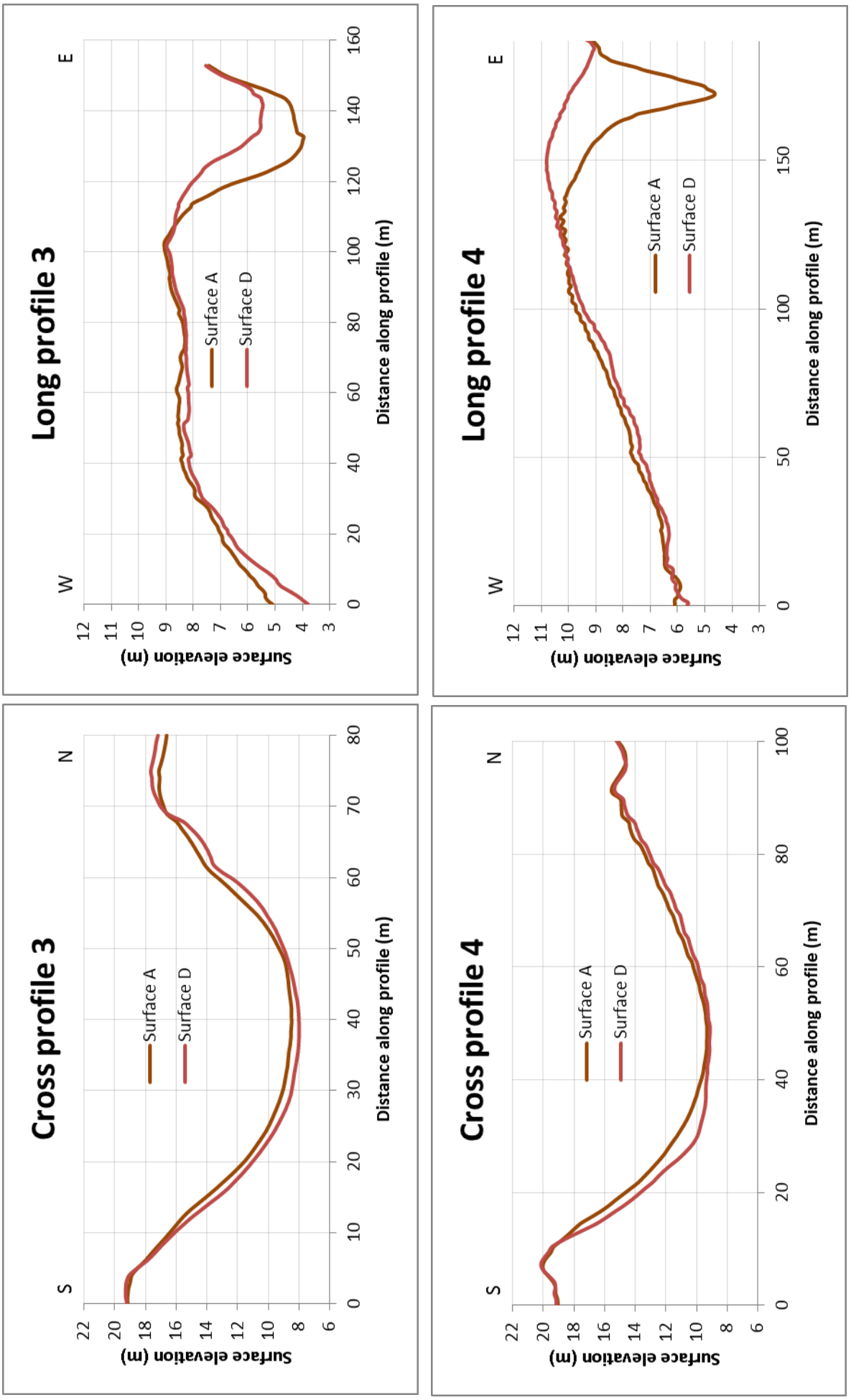

Figure 17. Cross and long profiles of trench 3 and 4. Note longitudinal profile of trench 4, which is different from the other profiles.

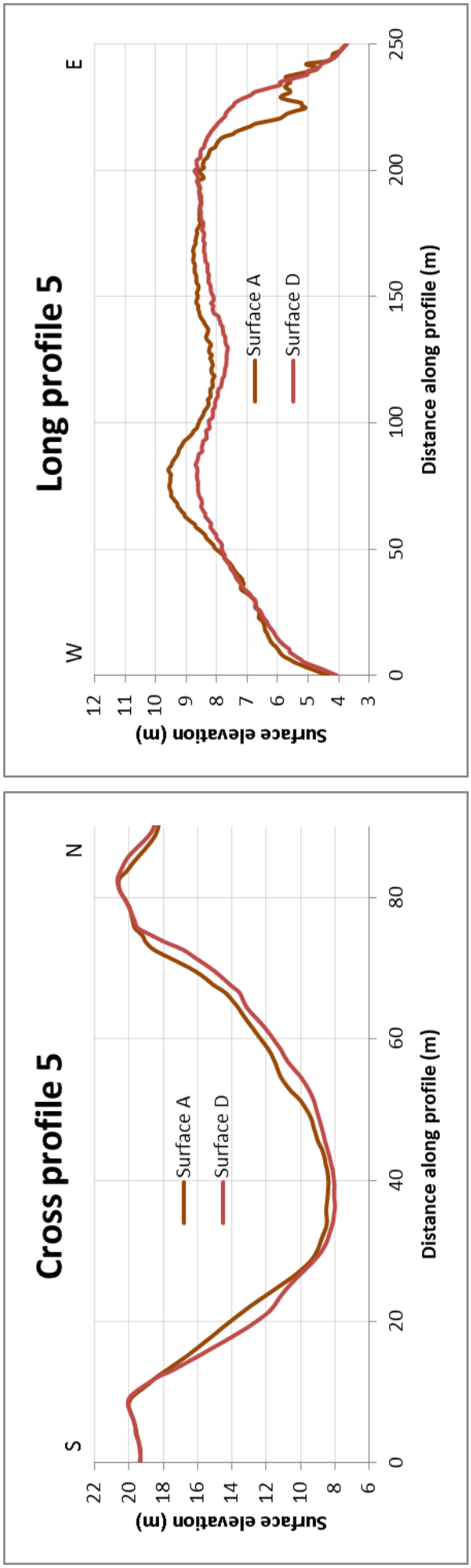

Figure 18. Cross and long profile of trench 5. In trench 5, location of the deflation basin is rather unclear, with the highest part being classified as deflation basin.

5. Discussion

5.1. Morphology and evolution

The man-made trenches at Zuid-Kennemerland all have a lower length to width ratio than would normally be expected for a natural trough blowout (i.e. they are relatively too wide). According to Hesp (2002), trough blowouts grow towards a threshold size as they become too wide to effectively steer and accelerate airflow. Although no further specification is given in terms of a length to width ratio, the trenches at Zuid-Kennemerland could have reached a threshold size based on their dimensions alone (Table 1). It should be noted that these trenches were made this way, and that their potential threshold size is not the result of an evolutionary trend. On the other hand, no significant revegetation occurred during the one-year measuring period, suggesting that the blowouts have not yet reached the evolutionary stage of an incipient blowout.

The sidewalls of the trenches do not retreat due to oversteepening as opposed to sidewalls in a natural trough blowout (see e.g. Carter *et al.*, 1990; Gares, 1992). Instead, the sidewalls of all trenches become steeper over time and stay in a fixed position, suggesting that they have not yet reached the material's angle of repose. Some steeper sections near the uphill margin of the sidewalls are stabilized by vegetation. The apparent stability of the sidewalls suggests that sediment is picked up from the sidewalls directly, rather than that sediment is transported downhill due to mass wasting. This view also agrees with the general lack of deposits (e.g. in a slump toe) downhill of the sidewalls and on the deflation basin margins. However, it is still possible that in between the measurements, some sediment from the sidewalls was transported onto the deflation basin and was subsequently removed. I suggest that, if the steepening of the sidewalls continues, the sidewalls will eventually start to retreat. This theory is supported as the first sign of sidewall retreat is visible on the southern sidewall of trench 2 (Figure 16). Following this theory, I expect that the frequency and magnitude of sidewall mass wasting events will increase. This will lead to a more natural sidewall-deflation basin interaction, in which sediment is removed from the sidewalls, transported onto the deflation floor, and moved out of the trough from there (cf. Gares, 1992; Hesp and Hyde, 1996; Hesp, 2002).

In a natural trough blowout, there is a clearly distinguishable transportational ramp that connects the deflation basin with the active, downwind part of the depositional lobe. The depositional lobe itself is typically located at a higher elevation than the deflation basin (see examples in e.g. Hesp and Hyde, 1996; Hesp, 1996; Byrne, 1997; Fraser *et al.*, 1998; Neal and Roberts, 2001; Hesp, 2002; Pease and Gares, 2013; Smyth *et al.* 2014). The trenches at Zuid-Kennemerland show distinctly different depositional lobe morphology. There is no clear transportational ramp. The area between the deflation basin and the depositional lobe is a gentle slope followed by an unpronounced depositional lobe crest, which barely lies more than 0,5 m above the level of the deflation floor (see profiles, Figure 16,Figure 17 Figure 18). The depositional lobes develop behind the foredune, inside the damp dune valley. Hence, the active lobe part lies at a considerably lower elevation than the lowest point of the deflation floor. This is in stark contrast with depositional lobes that are part of the foredune (e.g. Hesp and Hyde, 1996; Fraser *et al.*, 1998; Hesp and Pringle, 2000; Pease and Gares, 2013) or those that become an elevated part of the foredune crest (e.g. Smyth *et al.*, 2014). In all of these examples, the trough blowout has expanded into the foredune, but never cut all the way through. Hence, the depositional lobe is superimposed on a former part of the foredune. The complete lack of a clear boundary region (i.e. transportational ramp), depositional lobe crest and elevated active lobe makes it hard to distinguish these features in the field. Only by using the change maps, the active lobe is visualized as an area of deposition. I conclude that especially the landward portion of the man-made trenches does not resemble natural trough blowout morphology. Instead, the trenches have been cut all the way through the foredune, leaving the damp dune valley behind it as a huge sink for the depositional lobes to develop in.

Depositional lobe length does not correlate with deflation basin length in the almost 1:1 ratio found by Hesp (2002). However, the depositional lobes have expanded over time and may continue to grow in length as time progresses. The relatively small size of the depositional lobes is best explained by their location. Most of the sediment carried from and through the trench is immediately deposited behind the deflation basin (i.e. in the dune valley behind the foredune ridge), possibly due to a sudden increase of vegetation roughness in the densely vegetated dune valley (cf. Anderson and Walker, 2006). This leads to the development of a relatively short active lobe that features rapid vertical expansion. The predominant vertical expansion of the lobe is also reflected by the sudden, steep landward boundary of the depositional lobe. Another explanation is the lack of a transportational ramp followed by a depositional lobe crest. The transportational ramp, lobe crest and lee-side active lobe behave very much like a regular dune (Hesp and Hyde, 1996; Hesp, 1996). Flow acceleration and separation over the lobe crest will most likely cause the sediment to spread out more due to variation in grain fall velocities. In Zuid-Kennemerland, no flow separation and subsequent grain fall takes place. Grains transported as bedload settle in-situ if flow velocity becomes critically low and thus deposits cover only a small area. I theorize that expansion of the depositional lobes will continue, but will never reach the 1:1 ratio of a natural trough blowout because

the sediment is promoted to stack up, rather than to spread out.

5.2. Implications on flow dynamics and form-flow relation

There is a clear correlation between dominant wind direction/speed (Figure 10) and erosion within the troughs. Dominant and relatively strong southwestern winds correspond with accelerated erosion rates in the deflation basins during time period B-C. Interestingly, the sidewalls show an opposite trend during this period that cannot be explained by ambient wind conditions. However, sidewall erosion is not completely unrelated to ambient wind conditions. I suggest that preferential erosion of the northern sidewall in period B-C was due to the dominant southwestern winds. Under these circumstances, airflow enters a trench from the southwest and reflects off the northern sidewall. The southern sidewall remains protected from direct impact of airflow, whereas accelerated airflow reflecting off the northern sidewall results in the removal of sediment if flow-induced shear stress is great enough. The sidewall reflection possibly results in an S-shaped main jet inside the trough conform the findings of Pease and Gares (2013). A second possibility is that airflow separates over the southern rim at certain oblique approach angles and reattaches further down in the deflation basin or on the northern sidewall. This results in a helicoidal flow (flow reversal cell) under the separated flow (cf. Fraser *et al.*, 1998; Hesp and Pringle, 2001; Pease and Gares, 2013). This would result in dominant northern sidewall erosion and possibly more deposition on the southern sidewall as the reversed flow is able to carry sediment from the deflation basin onto the sidewall. This theory is supported by the relatively large areas of deposition on the southern sidewalls during period B-C.

The migration direction and growth of the depositional lobes during the one-year period is related to local airflow direction and magnitude. Position of the active lobe is mostly along the blowout axis (i.e. trench 2, 4 and 5) or slightly offset to the north (i.e. trench 1 and 3). All active lobes seem to migrate in ENE direction. The migration direction is a result of the jet flow leaving the trough. The offset position of some of the active lobes could be explained by the S-shaped flow pattern, causing airflow to leave the trough at an angle. Another possibility is that ambient airflow separates over the adjacent sidewall or foredune ridge and alters the migration direction of the active lobe. Based on active lobe dimensions and longitudinal profile, the outflow pattern seems to correspond to axial jet outflow of a distributary mouth (trench 2 and 4) or plane turbulent jet diffusion (trench 1, 3 and 5) to some extent. A similar comparison with river outflow patterns was first suggested by Hesp (1982), cited by Hesp (2002). However, in the review of Hesp (2002), he concluded that airflow leaving a blowout is far more complex than flow leaving a river mouth, thus making the analogy incorrect from a flow dynamics point of view.

Variation in active lobe dimensions relates to flow conditions and shows a seasonal trend. In period A-B the active lobe area is relatively small. In period B-C the active lobes develop a parabolic shape and migrate further to the northeast. I suggest that the parabolic shape is related to more frequent and stronger southwestern winds during this period, following the theory of lateral spreading on the transportational ramp (Hesp and Hyde, 1996; Fraser *et al.*, 1998; Hesp, 2002). In period C-D, large areas in front of the former active lobe are reactivated as sediment is less likely to reach the maximum extent of the active lobe due to weaker flow velocities. Although measurements only span a single year, the variation in active lobe shape and size due to flow conditions may also show an evolutionary trend. It appeared that the active lobe area increased in size between each consecutive period by comparison of Figure 15a,Figure **15**b and 15c. Since the depositional lobes have filled up the area directly behind the trough, a new fan-shaped platform was created that connects the trough with the dune valley. I expect that sediment can be transported further away from the trough over this platform, hence increasing the surface area where sediment is deposited.

The implications of length-width ratio on flow dynamics remain unclear. It is also unclear whether the suggested treshhold size by Hesp (2002) has been reached by any of the trenches. The blowout investigated by Hesp and Pringle (2001) has a l:w ratio of about 2:1 and supposedly steers winds approaching at an angle of 100° with respect to the blowout axis into the blowout. In the more recent studies of Pease and Gares (2013) and Smyth *et al.* (2014), trough blowouts with a l:w ratio of about 2,5:1 effectively steer wind parallel to its axis at approach angles of up to 50°. These results are contradictive and hence, only assumptions can be made with regards to the critical approach angle. Therefore, it is difficult to say whether topographical steering and jet formation takes place in any of the trenches without doing further field experiments. However, erosional and depositional patterns derived from this remote sensing study in combination with existing literature do provide a very rudimentary insight into flow dynamics. Trench 1 is probably too wide to effectively steer ambient airflow into the blowout and parallel to its axis. This is reflected by the wide depositional lobe and its fast northward migration, almost perpendicular to the blowout axis. Thus, based on the morphological development of trench 1, it is reasonable to expect that the critical approach angle for jet formation is lowest for trench 1. For all other trenches, the active lobe area is better aligned with the blowout axis. In addition there is almost no (noticeable) rim dune deposition or spillover lobe formation, suggesting that flow inside the trough is generally well contained and roughly steered

parallel to the blowout axis under a wider range of approach directions.

During the one year period, variation in basin, sidewall and active lobe deposition or erosion rate decreased when comparing all five trenches. The decreasing variance could indicate that the systems are working towards an equilibrium situation. This could mean that the trenches become more similar as they take the form of a more natural trough blowout. However, the time span of the measurements is too short to draw a solid conclusion. The trend in variance could repeat itself every year if it is tied with dominant wind conditions. It is also possible that the decreasing trend in variance is a coincidence.

5.3. Usability of the remote sensing technique

The use of remote sensing techniques and modern software such as Agisoft, ArcGis and SAGA allow for a very efficient and accurate description of morphological changes. Accuracy is limited to a certain degree by the resolution of the DEM. The 1x1 m resolution fails to capture every small-scale detail, such as developing rim dunes. However, for quantification of erosion and deposition rates in areas spanning 10s to 100s of meters, the 1x1 m resolution is more than sufficient.

The manual classification technique used in this study is a potential source of errors and inaccuracy. Even if clear boundary conditions for each class are given, the actual classification remains rather subjective. In addition, the trenches at Zuid-Kennemerland were classified according to morphological features of natural trough blowouts, whereas it appeared that the trenches lack some of these features. Hence, the classification process is complicated and prone to small errors. The results of this study are precise and are therefore suitable for comparison with each other (e.g. northern vs southern sidewall erosion). However, data from this study is less useful when comparing to data from other quantitative studies in the same area.

Results may also be influenced by human activities. Trench 1 is open to the public and is actively maintained to prevent facilities such as public bicycle paths from getting covered by sand. Sand from its depositional lobe is often relocated to the beach or to the blowout mouth. The latter explains the sudden deposition of sediment in front of trench 1 (visible on Figure 15). Other smaller scale effects of human activity, such as trampling, may slightly alter results, especially those of trench 1.

The goal of this study is to combine the remotely sensed data with our current knowledge of trough blowout flow dynamics. Even if the trenches at Zuid-Kennemerland were morphologically identical to natural trough blowouts, there would still be too much uncertainty to give an accurate overview of their internal flow dynamics. Based on literature and my own observations I conclude that a generalized and very rudimentary idea of trough blowout flow dynamics can be established based on remotely sensed morphological development and environmental setting. However, the comparison of numerous quantitative studies on trough blowouts shows that flow dynamics and sediment transport is highly variable due to a multitude of causes. This emphasizes the importance of empirical research to gain quantitative knowledge of each individual blowout's flow dynamics.

6. Conclusions

The man-made trenches at Zuid-Kennemerland do not resemble natural trough blowouts from a morphological and an evolutionary point of view. There are four major differences:

(1) The length-to-width ratio of the trenches is considerably lower than that of natural trough blowouts
(2) The natural sidewall-deflation basin interaction, wherein the sidewalls retreat and deliver sediment to the deflation basin, has not yet been established. However, it is expected that this interaction will be established in the near future.
(3) Most depositional lobes are located behind the foredune ridge and inside the heavily vegetated damp dune valley. This causes a distinctly different depositional lobe development dominated by vertical growth.
(4) There is no clear transportational ramp or depositional lobe crest in any of the trenches, which affects lobe development and sediment transport.

Since the trenches do not adhere to natural trough blowout morphology, no solid conclusions can be drawn regarding primary and secondary flow dynamics based on current trough blowout studies. However, there is a clear correlation with ambient wind conditions, giving a rudimentary insight into flow dynamics.

(1) Erosion of the deflation basin is greatest during winter, when strong southwestern winds dominate. Northern sidewall preferential erosion also concurs with strong southwesterly winds.
(2) Active lobe migration and size variation is also related to ambient wind conditions and possibly shows a seasonal trend. During periods with strong southwestern ambient winds, the lobe is small, active (deposition-wise) and of parabolic shape. If ambient winds become calmer, the lobe covers a larger area, does not necessarily has a parabolic shape and is less active in terms of deposition rate.

(3) The trenches are capable of topographically steering oblique incident winds. Airflow within the trough seems to be well-contained as there is no evidence of flow separating over the rim, leaving the trough. However, no good estimates of critical approach angle for topographical steering could be made.

Flow dynamics within the troughs remain largely unexplained as the Zuid-Kennemerland trenches cannot be compared to natural trough blowouts. A field study is required to gain better knowledge of flow dynamics within the trenches.

Acknowledgements

I would like to thank Prof. Dr. Gerben Ruessink for his support and efforts to provide me with all DEMs. I thank the Royal Dutch Meteorological office for freely providing historical meteorological data through their website. Finally, I thank Ir. C. van Onselen for converting and organizing wind vector and speed data.

References

Adamson, D., P. Selkirk & E. Colhoun. (1988). Landforms of aeolian, tectonic and marine origin in the bauer bay-sandy bay region of subantarctic macquarie island. Paper presented at the Papers and Proceedings of the Royal Society of Tasmania, , 122(1) pp.65-82.

Anderson, J.L. & I.J. Walker. (2006), Airflow and sand transport variations within a backshore-parabolic dune plain complex: NE Graham Island, British Columbia, Canada. Geomorphology 77(1-2), pp.17-34.

Arens, S.A., H.M.E. van Kamm-Peters & J.H. van Boxel. (1995), Airflow over foredunes and implications for sand transport. Earth Surface Processes and Landforms 20(4), pp.315-332.

Arens, S.M., J.P. Mulder, Q.L. Slings et al. (2013), Dynamic dune management, integrating objectives of nature development and coastal safety: examples from the Netherlands. Geomorphology 199, pp.205-213.

Arens, S., Q. Slings & C. De Vries. (2004), Mobility of a remobilised parabolic dune in Kennemerland, The Netherlands. Geomorphology 59(1), pp.175-188.

Baddock, M.C., G.F. Wiggs & I. Livingstone. (2011), A field study of mean and turbulent flow characteristics upwind, over and downwind of barchan dunes. Earth Surface Processes and Landforms 36(11), pp.1435-1448.

Battiau-Queney, Y. (2014), The dunes of Merlimont (North of France): a natural museum of aeolian landforms. Dynamiques Environnementales - Journal international des géosciences et de l'environnement 33(1), pp.51-64.

Bird, E.C.F. (1974), Dune stability on Fraser Island. Naturalist 21, pp.15-21.

Byrne, M.-. (1997), Seasonal sand transport through a trough blowout at Pinery Provincial Park, Ontario. Canadian Journal of Earth Sciences 34(11), pp.1460-1466.

Carter, R. W. G. (1988). Coastal Environments. London: Academic Press.

Carter, R.W.G., P.A. Hesp & K.F. Nordstrom. (1990). Erosional landforms in coastal dunes. In K. F. Nordstrom, N. P. Psuty & R. W. G. Carter (Eds.), Coastal Dunes: Form and Processespp. 217-250. Chichester: Wiley.

Dech, J.P., M.A. Maun & M.I. Pazner. (2005), Blowout dynamics on Lake Huron sand dunes: Analysis of digital multispectral data from colour air photos. Catena 60(2), pp.165-180.

Fraser, G.S., S.W. Bennett, G.A. Olyphant et al. (1998), Windflow circulation patterns in a coastal dune blowout, south coast of Lake Michigan. Journal of Coastal Research 14(2), pp.451-460.

Gares, P.A. (1992), Topographic changes associated with coastal dune blowouts at Island Beach State Park, New Jersey. Earth Surface Processes and Landforms 17(6), pp.589-604.

Gares, P.A. & K.F. Nordstrom. (1995), A cyclic model of foredune blowout evolution for a leeward coast: Island Beach, New Jersey. Annals - Association of American Geographers 85(1), pp.1-20.

González-Villanueva, R., S. Costas, H. Duarte et al. (2011), Blowout evolution in a coastal dune: Using GPR, aerial imagery and core records. Journal of Coastal Research(SPEC. ISSUE 64), pp.278-282.

Halls, R.J. & J. Bennett. (1981), Wind and sediment movement in coastal dune areas. IN: PROC.SEVENTEENTH COASTAL ENGNG.CONF., (SYDNEY, AUSTRALIA: MAR.23-28, 1980) 2 , New York, U.S.A., Am. Soc. Civ. Engrs., 1981, Part 2, Chapter 94, pp.1565-1575.

Hesp, P.A. (1982). Morphology and Dynamics of Foredunes in S.E. Australia. Unpublished PhD Thesis, Dept. Geography. University of Sydney, 397 pp.

Hesp, P.A. & A. Pringle. (2012), Flow behaviour in a trough blowout. Tangimoana, New Zealand. Journal of Coastal Research 34(SI), pp.597-601.

Hesp, P.A. & A. Pringle. (2001), Wind flow and topographic steering within a trough blowout. Journal of Coastal Research, pp.597-601.

Hesp, P. (2002), Foredunes and blowouts: initiation, geomorphology and dynamics. Geomorphology 48(1-3), pp.245-268.

Hesp, P.A. (1996), Flow dynamics in a trough blowout. Boundary-Layer Meteorology 77(3-4), pp.305-330.

Hesp, P.A. & R. Hyde. (1996), Flow dynamics and geomorphology of a trough blowout. Sedimentology 43(3), pp.505-525.

Hugenholtz, C.H. & S.A. Wolfe. (2006), Morphodynamics and climate controls of two aeolian blowouts on the northern Great Plains, Canada. Earth Surface Processes and Landforms 31(12), pp.1540-1557.

Hugenholtz, C.H. & S.A. Wolfe. (2009), Form-flow interactions of an aeolian saucer blowout. Earth Surface Processes and Landforms 34(7), pp.919-928.

Jackson, D.W.T., J.H.M. Beyers, K. Lynch et al. (2011), Investigation of three-dimensional wind flow behaviour over coastal dune morphology under offshore winds using computational fluid dynamics (CFD) and ultrasonic anemometry. Earth Surface Processes and Landforms 36(8), pp.1113-1124.

Javernick, L., J. Brasington & B. Caruso. (2014), Modeling the topography of shallow braided rivers using Structure-from-Motion photogrammetry. Geomorphology 213, pp.166-182.

Jungerius, P.D., A.J.T. Verheggen & A.J. Wiggers. (1981), The development of blowouts in ' De Blink', a coastal dune area near Noordwijkerhout, the Netherlands. Earth Surface Processes & Landforms 6(3-4), pp.375-396.

Klijn, J. (1990), The younger dunes in the Netherlands; chronology and causation. Dunes of the European coasts: geomorphology–hydrology–soils.Catena Supplement 18, pp.89-100.

KNMI. (2008). De toestand van het klimaat in Nederland 2008 (The state of the climate in the Netherlands 2008). De Bilt: Royal Dutch Meteorological Office.

Kuipers, M. (2014), The daring Dutch: restoring the dynamic dunes. Dynamiques Environnementales - Journal international des géosciences et de l'environnement 33(1), pp.132-138.

Lynch, K., D.W. Jackson & J.A.G. Cooper. (2010), Coastal foredune topography as a control on secondary airflow regimes under offshore winds. Earth Surface Processes and Landforms 35(3), pp.344-353.

Marta, M.D. (1958). Coastal dunes: A study of the dunes at vera cruz. 6th Coastal Engineering Conf. ASCE, New York, pp.520-530.

Neal, A. & C.L. Roberts. (2001), Internal structure of a trough blowout, determined from migrated ground-penetrating radar profiles. Sedimentology 48(4), pp.791-810.

Parsons, D.R., I.J. Walker & G.F. Wiggs. (2004), Numerical modelling of flow structures over idealized transverse aeolian dunes of varying geometry. Geomorphology 59(1), pp.149-164.

Pease, P. & P. Gares. (2013), The influence of topography and approach angles on local deflections of airflow within a coastal blowout. Earth Surface Processes and Landforms 38(10), pp.1160-1169.

Provoost, S., M.L.M. Jones & S.E. Edmondson. (2011), Changes in landscape and vegetation of coastal dunes in northwest Europe: a review. Journal of Coastal Conservation 15(1), pp.207-226.

Smyth, T.A.G., D. Jackson & A. Cooper. Airflow and aeolian sediment transport patterns within a coastal trough blowout during lateral wind conditions. Earth Surface Processes and Landforms 39(14), pp.1847-1854.

Smyth, T.A.G., D.W.T. Jackson & J.G. Cooper. (2013), Three dimensional airflow patterns within a coastal trough-bowl blowout during fresh breeze to hurricane force winds. Aeolian Research 9, pp.111-123.

Thom, B., P. Hesp & E. Bryant. (1994), Last glacial "coastal" dunes in Eastern Australia and implications for landscape stability during the Last Glacial Maximum. Palaeogeography, Palaeoclimatology, Palaeoecology 111(3-4), pp.229-248.

Walker, I.J., P.A. Hesp, R.G. Davidson-Arnott et al. (2006), Topographic steering of alongshore airflow over a vegetated foredune: Greenwich Dunes, Prince Edward Island, Canada. Journal of Coastal Research, pp.1278-1291.

Walker, I.J. & W.G. Nickling. (2002), Dynamics of secondary airflow and sediment transport over and in the lee of transverse dunes. Progress in Physical Geography 26(1), pp.47-75.

Wang, S., E. Hasi, J. Zhang et al. (2007), Geomorphological significance of air flow over saucer blowout of the Hulun Buir sandy grassland Journal of Desert Research 27, pp.745-749.

Whitney, J.W., G.N. Breit, S.E. Buckingham et al. (2015), Aeolian responses to climate variability during the past century on Mesquite Lake Playa, Mojave Desert. Geomorphology 230, pp.13-25.